E-Infrastructures

H2020-EINFRA-2015-1

EINFRA-5-2015: Centres of Excellence

for computing applications

EoCoE

Energy oriented Center of Excellence

for computing applications

Grant Agreement Number: EINFRA-676629

D5.5 M36

Towards ITER relevant simulations

D5.5 M36 Towards ITER relevant simulations

Project and Deliverable Information Sheet

EoCoE	Project Ref:	EINFRA-676629
	Project Title:	Energy oriented Centre of Excellence
	Project Web Site:	http://www.eocoe.eu
	Deliverable ID:	D5.5 M36
	Lead Beneficiary:	CEA
	Contact:	Yanick SARAZIN
	Contact's e-mail:	yanick.sarazin@cea.fr
	Deliverable Nature:	Report
	Dissemination Level:	PU
	Contractual Date of Delivery:	M36 30/09/2018
	Actual Date of Delivery:	M36 20/09/2018
	EC Project Officer:	Carlos Morais-Pires

* - The dissemination level are indicated as follows: PU – Public, CO – Confidential, only for members of the consortium (including the Commission Services) CL – Classified, as referred to in Commission Decision 2991/844/EC.

Document Control Sheet

Document	Title :	Towards ITER relevant simulations
	ID :	D5.5 M36
	Available at:	http://www.eocoe.eu
	Software tool:	Microsoft Word
Authorship	Written by:	Yanick SARAZIN Marina BECOULET, Guilhem DIF-PRADALIER, Guillaume LATU, Patrick TAMAIN
	Contributors:	Virginie GRANDGIRARD
	Reviewed by:	E. Audit, N. Girard, PEC members

This deliverable deals with the progresses regarding our physics understanding of core turbulence and transport, Edge Localized Modes (ELMs) and their control, and heat and particle exhaust at the periphery of tokamak plasmas. The considered issues have explored regimes of parameters which lie in the ITER relevant range. They have been permitted by numerical upgrades – permitted by dedicated works of WP1, and point-to-point interactions with WP1 – of the HPC codes GYSELA (5-dimensional gyrokinetic), JOREK (3D resistive MHD) and TOKAM3X (3D multi-fluid), respectively.

1. Progress in core transport modelling using the 5-dimensional GYSELA code

1.1. Introduction

Turbulence governs heat confinement in tokamak fusion plasmas. In turn, turbulence properties explain why large machines, like ITER, are required so as to reach the desired performance in terms of energy gain. Understanding, predicting and possibly controlling turbulent transport is therefore of outermost importance in fusion research. In addition to experimental measurements, High Performance Computing (HPC) allows one to gain much insight in these critical issues.

In standard regimes of plasma confinement, turbulence is mainly electrostatic (fluctuations of the magnetic field can be neglected) and develops at spatial scales of the order of a few ion Larmor radii (i.e. of the order of one centimeter) in the plane transverse to the guiding magnetic field, and of the order of the machine size (several meters) along the magnetic field lines. Turbulence typical frequencies range from a few to a few hundreds of kHz, i.e. orders of magnitudes below the ion cyclotron frequency. One of the striking properties of these small-scale small-amplitude fluctuations is to generate large scale low frequency flows, which efficiently contribute to turbulence saturation. These zonal flows are linearly damped by collisions only [Diamond 2005]. In addition, turbulent transport has been shown to exhibit large scale transport events, called avalanches, leading to the ballistic propagation of particles, momentum and heat on radial distances much larger than the turbulence correlation length [Diamond 1995, Garbet 1998, Sarazin 1998]. Both zonal flows and avalanches highlight the intrinsic multiscale nature of turbulence self-organization, where disparate scales and plasma regions interact with each other [Dif-Pradalier 2010].

Owing to their high temperature and low density, tokamak fusion plasmas are weakly collisional. As a consequence, they require a kinetic description which is *a priori* 6-dimensional (3D in position, 3D in velocity). Fortunately, turbulence can be solved within the so-called 5D (3D in position, 2D in velocity) gyrokinetic framework, whereby phase space reduction is obtained by filtering out the fast gyro-motion. The GYSELA code solves the gyrokinetic equation self-consistently coupled to the quasi-neutrality [Grandgirard 2016]. The full distribution functions of the gyro-centers $f_s(r,\theta,\varphi,v_{//},\mu,t)$ are evolved in time under the forcing of prescribed sources (of heat, momentum, *etc.*). Here, r is the direction of confinement (radial), θ and φ are the poloidal and toroidal angles of the torus, $v_{//}$ is the parallel velocity and μ is the adiabatic invariant (ratio of the transverse kinetic energy of the particles over the strength of the magnetic field). As discussed later, Coulomb collisions also reveal important and are accounted for in GYSELA.

In the path towards ITER relevant simulations, critical bottlenecks of two different natures have been overcome in the course of the EoCoE project.
The first one deals with the capability to run simulations at dimensionless parameters close to the ones expected in ITER. This is particularly critical regarding ρ_*, the ratio of the ion Larmor radius over the machine size. On the one hand, empirical scaling laws report that the energy confinement time strongly depends on this parameter [ITER 1999]. On the other hand, simulations have shown that the scaling exponent converges at small enough ρ_* only [Lin 2002, McMillan 2010, Sarazin 2011]. The point is that the number of grid points typically scales like $\rho_*^{-\alpha}$, with $2<\alpha<3$ depending on the numerical scheme. In ITER, ρ_* is expected to be of the order of 2.10^{-3}, a factor of two smaller than in the actual largest machines. Small ρ_* simulations have been permitted thanks to the constant upgrade of code performance in terms of parallelization and memory footprint. Also, the previous α exponent has been brought back to 2 by using a "field aligned" method detailed in section 1.2.
The second one deals with the richness of the implemented physical model. In that respect, three major upgrades have been achieved within EoCoE. First (cf. section 1.3), kinetic electrons are now implemented, allowing for both the investigation of turbulent particle transport and of the ion-scale turbulence governed by a certain class of electrons. Second (cf. section 1.4), a novel linearized multi-species collision operator has been derived and successfully implemented, especially valid to account for ion-electron collisions. Third (cf. section 1.5), boundary layers have been critically refined, by removing the "mesh hole" in the very core of the tokamak, and by accounting for the unconfined peripheral region with open magnetic field lines.

1.2. The field aligned approach

In a tokamak, due to the large confining magnetic field, transport along the magnetic field lines is much faster than across them. In turn, a fast homogenization occurs along the magnetic field lines, leading to small variations in the parallel direction ($k_{//}$~qR, with q the safety factor and R the major radius). Conversely, the scale length of the fluctuations is much smaller (a few ion gyro-radii) in the perpendicular directions. Optimized simulations should take into account this strong anisotropy for improved efficiency. To this aim, field aligned coordinates are used. The basic idea is to use coordinates that follow field lines (see Fig. 1). With such coordinates, a flux tube (a tube with a surface parallel to the magnetic field **B**), which is bent by magnetic curvature and twisted by magnetic shear, is mapped onto a rectangular domain. However, this approach has the drawback of needing a non-conformal correction after one turn, either in the poloidal or in the toroidal direction, which yields a break of symmetry. More importantly, field-aligned coordinates become singular when approaching the separatrix (the boundary between closed and open field lines, separating the toroidally confined region from the region where field lines connect to solid surfaces) in a divertor configuration, with possible deleterious consequences on the robustness of the associated numerical algorithm.
A promising alternative, introduced by Hariri-Ottaviani [Hariri 2013] and very flexible with respect to the choice of coordinates, has been applied to a *fluid* model. The main idea is to

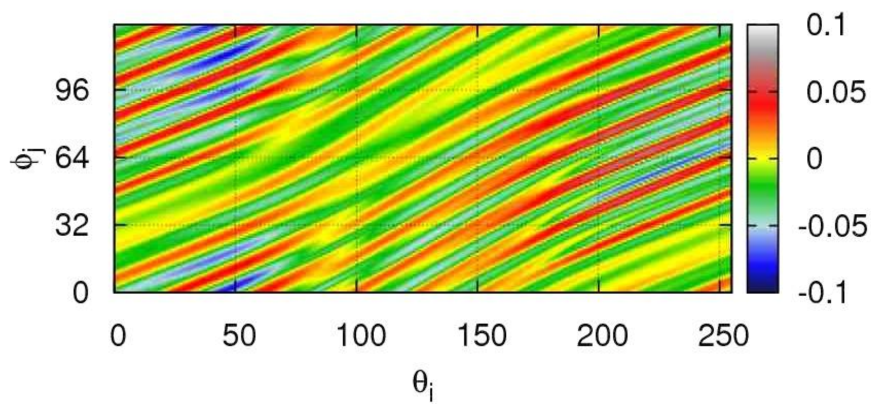

Figure 1: The aligned method aims at interpolating along the field lines exhibiting smooth variations of the various fields (electric potential here).

compute the parallel derivatives locally along the field lines, getting the needed values for finite differences by interpolating the intersection points of a field line with the poloidal planes.

Within EoCoE, we have performed a thorough numerical investigation of this idea in the context of *gyrokinetic* simulations using semi-Lagrangian methods. We have adapted and updated this method to the semi-Lagrangian context in conceiving a new interpolation operator. We have validated the method in several simplified settings and geometries. The strength of this scheme is that one can reduce genuinely the number of points in the longitudinal/parallel direction (along the field lines). As discussed below, numerical simulations show that field-aligned interpolation leads to considerable memory savings for the same level of accuracy. The scheme has been implemented in two semi-Lagrangian codes, Selalib and GYSELA, mainly considering the 4D gyrokinetic Vlasov equation in the zero-Larmor-radius limit, but also in 5D gyrokinetic simulations [Latu, 2018a]. In our benchmarks against the standard (non-aligned) scheme, we have observed large reductions in memory footprint, as well as a reduction of the number of points needed along toroidal direction, typically by a factor of 4 to 8. Our estimates suggested that these gains would be even larger in reactor-scale simulations (smaller ρ_* value). Actually, this so-called “field-aligned” method is now regularly employed in production runs, and some of them (especially with kinetic electrons) would have not been achievable without this upgrade of the code.

Field-aligned interpolation does not impose any constraint on the 2D poloidal grid, so that the use of magnetic flux coordinates (i.e. coordinates in the transverse plane which are tied to the magnetic flux surfaces) is not necessary. Accordingly, the magnetic axis (as well as the X-point in a divertor configuration) does not pose any theoretical problem. Therefore, the new scheme is well adapted to ITER relevant more complex magnetic geometries, including X-point and non-circular cross-sections of flux-surfaces. These will be considered in the near future within EoCoE-2.

We have designed robust parallel algorithms based on the aligned method that do not require an entire overhaul of the GYSELA code. As a matter of fact, we only needed to rewrite and adapt part of the Vlasov solver: the 1D advection along the φ direction was replaced by a 2D advection along both φ and θ directions. In addition, some extra communications were added, leading to small overheads. We also had to reconsider the estimate of the derivatives of some quantities along the φ direction with a specific method [Latu, 2018b].

There is a clear numerical gain of using the field-aligned method in GYSELA. We can typically run simulations with a quarter of the number of points along the φ direction with the aligned

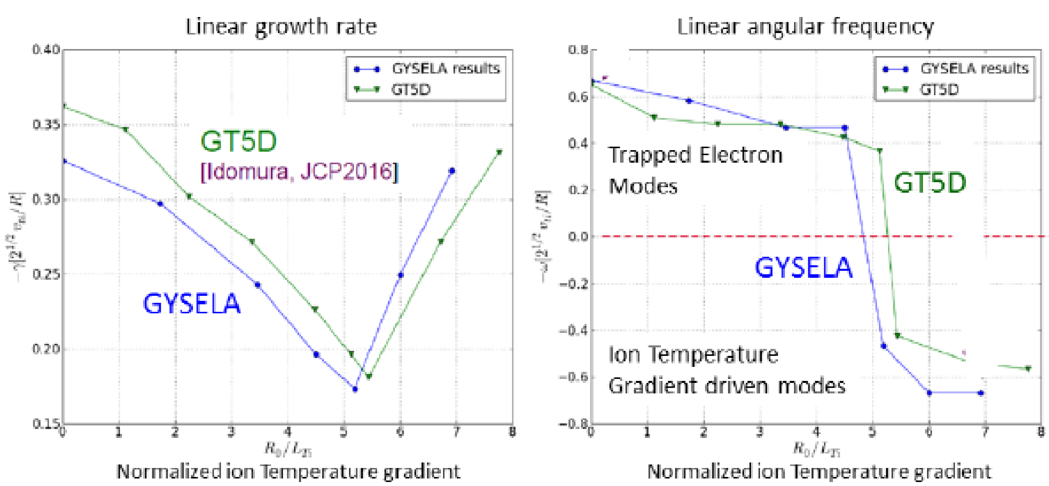

Figure 2: Linear growth rate and angular frequency of the most unstable mode as a function of the ion temperature gradient (the electron temperature gradient is kept fix (R_0/L_{Te} = 6.9).

method, while achieving the same accuracy as the non-aligned approach.

1.3. Kinetic electrons

At the start of EoCoE, the distribution function of the electrons was not solved in GYSELA. The electron kinetic response to ion-scale turbulence was modelled by assuming electrons respond adiabatically, exhibiting a Boltzmann response to electric field fluctuations. This assumption suffers however two major limitations: density and electric potential fluctuations being in phase, the predicted turbulent particle transport is vanishing in this framework; also, electron-driven

instabilities are inherently not accounted for in this model. In particular, this latter point prevents the study of trapped-electron mode (TEM) turbulence, which is expected to play a prominent role in electron heat transport in ITER relevant plasmas.
Accounting for electron dynamics in an ion-scale turbulence reveals challenging from the numerical point of view. Indeed, due to their low inertia, electrons move much faster than ions in the parallel direction, in the ratio $(m_i/m_e)^{1/2}$, m_s standing for the mass of the species. For deuterium plasma, this ratio is of the order of 60. Also, electron Larmor radius is smaller than that of the ions by the same ratio, so that the grid mesh should be adapted accordingly. All in all, accounting for kinetic electron physics might require increasing the amount of numerical resources by a factor $(m_i/m_e)^{\alpha/2}$, with $3<\alpha<4$, depending on the numerical scheme. Several strategies have been developed in GYSELA to keep this increase within acceptable limits. The first one is to focus on trapped electrons only. These exhibit larger characteristic transverse spatial scales than passing ones, hence requiring less grid points. More importantly, this class of electrons is the one responsible for TEM turbulence. Passing electrons are expected to play a critical role in advanced transport regimes exhibiting transport barriers, which are not the main focus of GYSELA simulations for the time being. The second one consists in considering artificially heavy electrons, hence reducing the ratio m_i/m_e and subsequently the numerical needs. This “trick” reveals particularly legitimate when studying TEM turbulence, since the instability mechanism relies on wave-particle resonance at a frequency which does not depend on the mass species. Third, we have developed the so-called field-aligned approach (see previous section), resulting in reducing the α exponent down to 3.
To this end, the kinetic treatment of electrons has been implemented in GYSELA. Two major modifications of the equations have been required. First, the drift-kinetic equation for the time evolution of the full distribution function of all (passing and trapped) electron gyro-centers is now solved at each time step, similarly to what is done for ions. Second, in the quasi-neutrality equation, the electron contribution is split in 2 terms: passing electrons are forced to respond adiabatically (as expected if they were be given the right small mass), while the electron distribution function is integrated over the trapped domain only to account for the kinetic response of trapped electrons. A dedicated treatment is performed for axisymmetric modes to prevent spurious high-frequency modes and preserve the zonal flow dynamics [Idomura 2016]. This upgraded version of GYSELA has been benchmarked in the linear regime of TEM by comparing to already published data. As reported on Fig. 2, one recovers the right magnitude and trends of both real frequency and growth rate of the most linearly unstable modes. Especially, the transition from the TEM to the ITG instability is observed when scanning the ion temperature gradient.

1.4. Linearized multi-species collision operator

Although fusion plasmas are weakly collisional, hence requiring a kinetic description, accounting for collisions in transport simulations is essential for at least three main reasons: (i) high collisionality reduces the time-life of those particles trapped in the local mirrors of the magnetic field along the field lines, leading to the reduction – up to the suppression – of trapped-particle-driven instabilities; (ii) the collisional friction exerted by these trapped particles on passing ones controls the low magnitude of the ion poloidal flow, known as the neoclassical flow; (iii) inter-species collisions are essential to account for impurity transport – off-diagonal cross-terms of the transport matrix play a critical role there – and collisional heat transfer processes.

At the start of EoCoE, a multi-species operator was operational in GYSELA. Its two major limitations were the following: operators in the adiabatic invariant μ were ignored so as to preserve the efficient parallelization in this direction, and critical assumptions were made on some of the relaxation frequencies so as to speed-up the operator. As a result, the expected relaxation of the distribution function towards a Maxwellian in the μ direction (Boltzmann's H theorem) was not ensured. Also, while the collision operator was valid for intra species collisions and trace impurities colliding on the main species, it was no longer valid for electron-ion collisions or for non-trace impurities.

These two limitations have been alleviated in the frame of EoCoE, with the analytical development, the implementation and the verification of a new collision operator.

Projecting the distribution function on a set of the orthogonal Laguerre polynomials allows one to replace the μ derivatives by analytical expressions. The projection requires to perform integrals in μ. Convergence tests have shown that a modest discretization in μ (64 points only) is required. Conversely, this treatment adds some analytical complexity to the problem, namely the projection of the collision operator on the polynomials. Regarding the characteristic relaxation frequencies, analytical fits have been obtained, leading to explicit integrals and derivatives which reveal much less numerically consuming. These results, including the benchmark with respect to the neoclassical theory, have been published and have given rise to several presentation in international conferences and meetings.

GYSELA is now one of the rare (if not the only one) codes in the world capable of addressing turbulent and collisional transport on an equal footing for any kind of 2-species simulations, including ion-electron, ion-impurity and ion-energetic particle.

In this framework, this new collision operator has been used to further study the transport of tungsten, one of the ITER-relevant impurities. It can be particularly deleterious to plasma confinement in cases where it accumulates in the core where it then radiates a large fraction of energy even at low concentrations. One of the critical issues here is to perform self-consistent simulations featuring both turbulent and neoclassical transport, so as to account for both possible competitions and synergies between these two transport channels. Such a dedicated highly resolved GYSELA simulation has been performed and analyzed. It appears that both poloidal

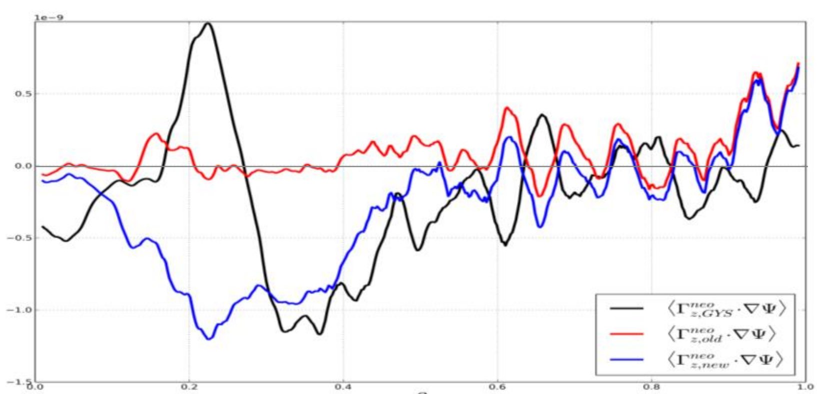

Figure 3: Comparison of the neoclassical contribution to the tungsten impurity flux coming from GYSELA (black), to neoclassical estimates according to the standard theory (red) and to the newly derived expression (blue) accounting for poloidal asymmetry and anisotropy of the tungsten pressure.

asymmetry and anisotropy of the impurity pressure governed by turbulence have a major impact on the neoclassical impurity flux. The correction terms to the standard neoclassical theory have been derived analytically, and found to be in fair agreement with the numerical results (cf. Fig. 3). This work provides a clear mechanism for synergy between neoclassical and turbulent processes in the context of impurity transport. A paper has been submitted, and several presentations given on the subject.

1.5. From the very core to the outer edge

Whenever using the polar coordinate system in a circular domain in the poloidal plane, one faces a numerical issue at the magnetic axis $r=0$. There are several artifacts near this location arising in the Field solver and also in computing displacements in the Vlasov solver. For these reasons, up to 2016, we were constrained to restrain the computation domain to $r>r_{min}$ with artificial boundary conditions at r_{min}. In addition to this difficulty, the gyroaverage operator close to this singularity point leads to significant parallel overheads [Bouzat, 2017]. We aimed at overcoming these issues with a set of adapted solutions near the magnetic axis for several operators. Two actions were undertaken. First, on a short time scale, we slightly modified the numerical methods in order to partly cure them and to be able to track the plasma dynamics near the axis [Latu, 2018b, Section 3.3.4]. Secondly, on a much longer time scale, we have initiated a study concerning a new reduced polar grid in order to get a comprehensive remedy [Bouzat, 2018].
At the same time, the simulated plasma domain has been extended up to the open field line region, the so-called Scrape-Off Layer (SOL), which is long known to interact with the confined plasma in both ways. To this end, a penalizing technique has been implemented and started being validated.

1.5.1. Improving GYSELA to remove r_{min} boundary condition

In the Vlasov solver, the issue related to $r\sim0$ is mainly located in the 2D advection step in the poloidal plane (r,θ). Indeed, one has to perform both the calculation of footprint locations of the backward trajectories, and interpolations at $r<r_{min}$ with enough accuracy. We chose to switch from the usual interpolation scheme near the magnetic axis to a bilinear interpolation using the (x,y) Cartesian coordinates, hence removing the singularity induced by polar coordinates at $r=0$. A simple mixing scheme is used to mix the standard interpolation method far from $r=0$ and the Cartesian approach near $r=0$. While solving the main problem, this approach has two drawbacks: (i) the bilinear interpolation is of low order, and (ii) the bridge between the two interpolation operators introduces small artifacts.
We also adapted the Field solver (Quasi-neutral Poisson solver) to cope with the singularity. Following the work of [Lai, 2001], we modified the proposed solution for a classical 2D Poisson problem to match our gyrokinetic framework. We no more have the Dirichlet nor Neumann boundary conditions at r_{min}. This eliminates spurious artifacts at this location on the electric potential. This latter point is critical for turbulence modeling. Differences between the previous and new solutions are highlighted in Fig. 4, zooming at a given time step on the region $r=0$.
These modifications of Vlasov and Field solvers have been implemented in GYSELA. The simulation accuracy turns out to be much improved.

1.5.2. Reduced grid to design a new GYSELA version

To overcome the remaining problems and permanently solve spurious phenomena which occur when using a large number of points close to the *r=0* location, one has to deeply and

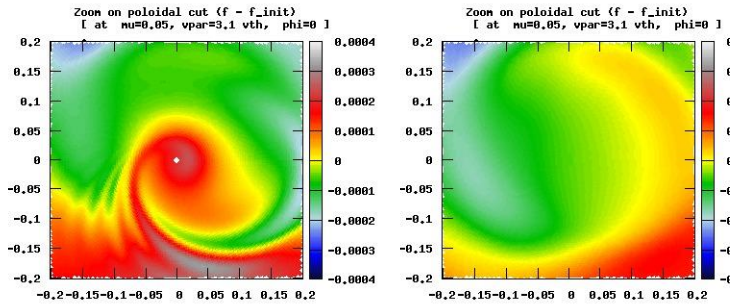

Figure 4: Snapshots of the distribution function in the 2D transverse pane (r,θ) close to the magnetic axis (r=0) with the original approach (polar coordinates, left) and with the new approach (Cartesian coordinates, right).

simultaneously modify the numerical schemes, the mesh and the code. To achieve this goal, the study has been performed on a simplified set of equations [Bouzat, 2018]. Our main purpose was to change the mesh of the poloidal plane while keeping a polar-like coordinate system. First, it would allow one to loosen the meshing in order to reduce the density of mesh-points near the magnetic axis. Second, the mesh should match the magnetic surfaces as much as possible. We then expect an improvement both in execution time by reducing the overall number of points, and in accuracy thanks to the grid being closer to the typical pattern of simulated phenomena. The new poloidal grid that we plan to use is depicted in Fig. 5.

In a more general perspective, the developed non-uniform meshing has also the advantage of allowing one to focus on a specific location of the plane that might require increased accuracy and more points (e.g. to address specific physical points), while the rest of the domain would remain unaffected elsewhere.

For each flux surface (with circular cross-section so far) labeled by the *r* coordinate, one can specify the number of points in the θ direction. This allows one to have either an uniform density of poloidal grid points, or to adapt this density to the required accuracy. This approach can be combined with a general mapping that changes the effective plasma shape, the polar mapping being only a special case. To shorten execution time, we have first restricted ourselves to mappings characterized by analytical formula, and whose inverse can also be expressed analytically. This is particularly relevant to describe advanced geometries of a tokamak, *e.g.* D-shaped plasma.

Several operators of the application have been re-designed to cope with non-uniform/reduced grid in the poloidal plane. This includes the interpolation operator with Lagrange polynomials, the gyroaverage operator and the quasi-neutral solver [Bouzat, 2018]. In addition, a diffeomorphism (mapping technique) has been developed and implemented to model relevant non-circular magnetic configurations. The positive results of this proof-of-concept study justifies

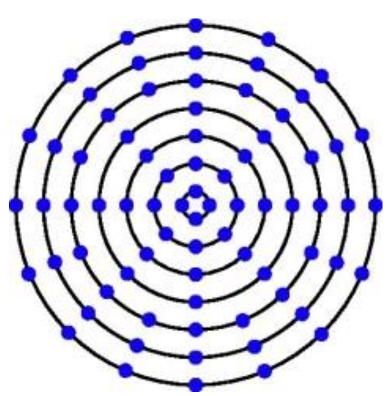

Figure 5: New poloidal mesh with a non-uniform grid along theta direction

that we should try to assemble these new components in a new GYSELA prototype in a near future [Latu, 2018b].

1.5.3. Penalizing technique for the open field line region (SOL)

We here report on a novel and more experimentally-relevant way to model the heat sink at the computation domain boundaries that aims at mimicking actual plasma-wall interaction. The computational domain is separated into a closed field line region (that of the confined core and edge) and a region where magnetic field lines intercept a material boundary (the so-called Scrape-Off Layer (SOL) region). This material boundary is comprised of two parts: one mimics the wall and is the farthest part of the domain; the other mimics a limiter akin to the one that has extensively been used in Tore Supra for heat and particle flux handling. This limiter is a solid material, toroidally symmetric and of given poloidal and radial extensions that protrudes from the plasma chamber. Both wall and limiter in GYSELA are now modeled as immersed boundaries through a penalization technique. A space-dependent mask function mimics the limiter and wall geometries within the simulation domain. A density-conserving Krook-restoring force is added to the gyrokinetic equation and acts on the above mask to drive the total distribution function towards target low temperatures, providing effective immersed heat sinks at the boundaries. Target sink distribution functions are chosen as low-temperature and low-density Maxwellians with both temperatures and densities typically 10 times smaller than that in the confined core plasma. The transition from immersed boundary to plasma is taken as sharp as numerical stability allows and typically occurs within a turbulence autocorrelation length. In that transition region, fluctuations of the distribution function are progressively damped and any heat flux arriving at the immersed boundaries is effectively removed from the system.

Illustrations are shown on Fig. 6, highlighting the geometry of a typical mask function and its use in flux-driven turbulent regimes in GYSELA for actual plasma parameters.

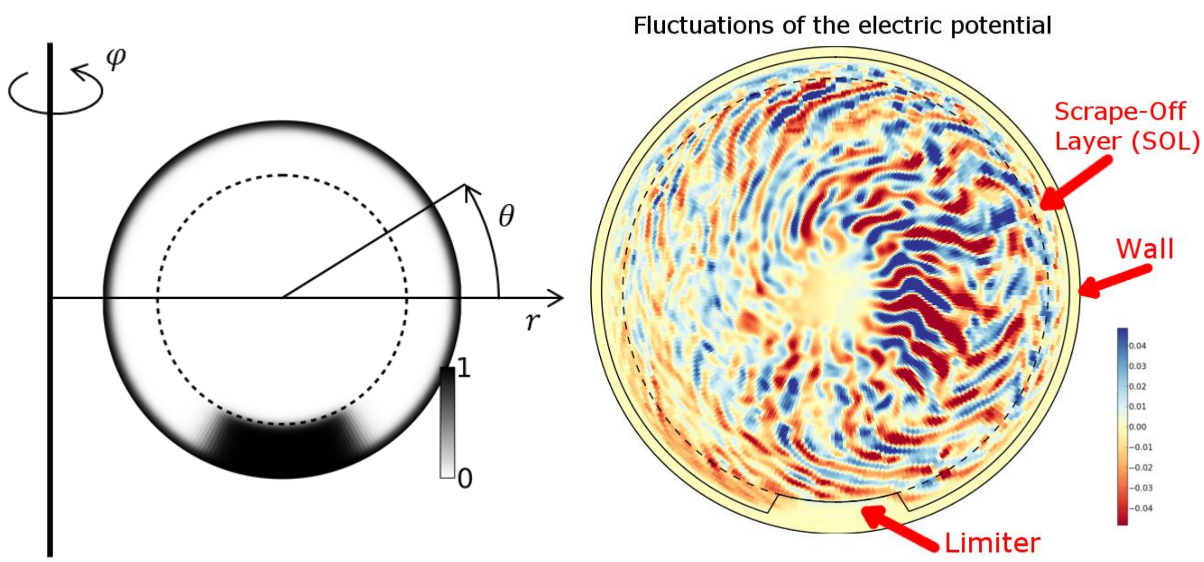

Figure 6: (Left) Poloidal section of the mask function; r is radius, θ and φ are respectively the poloidal and toroidal angles; the mask is axisymmetric (uniform along φ). The dotted circumference determines the separatrix between confined (closed field lines) and SOL (open field lines) regions. (Right) Core-edge-SOL combined calculation in GYSELA for Tore Supra-like parameters, in a turbulent regime with a penalized limiter. The modification of the characteristics of turbulence next to the transition from closed to open field lines is under current investigation.

1.6. References

[Bouzat, 2017] N. Bouzat, F. Rozar, G. Latu, J. Roman, ISPDC 2017 Proc. (2017) https://doi.org/10.1109/ISPDC.2017.12

[Diamond 1995] P.H. Diamond, T.S. Hahm, Phys. Plasmas 2 (1995) 3640

[Diamond 2005] P.H. Diamond, S.I. Itoh, K. Itoh, T.S. Hahm, Plasma Phys. Control. Fusion 47 (2005) R35

[Dif-Pradalier 2010] G. Dif-Pradalier, P. H. Diamond, V. Grandgirard, Y. Sarazin, J. Abiteboul, X. Garbet, Ph. Ghendrih, A. Strugarek, Phys. Rev. E 82 (2010) 025401 (R)

[Garbet 1998] X. Garbet, R. Waltz, Phys. Plasmas (1998)

[Grandgirard 2016] V. Grandgirard, J. Abiteboul, J. Bigot, T. Cartier-Michaud, N. Crouseilles, Ch. Ehrlacher, D. Estève, G. Dif-Pradalier, X. Garbet, Ph. Ghendrih, G. Latu, M. Mehrenberger, L. Mendoza, C. Norscini, Ch. Passeron, F. Rozar, Y. Sarazin, A. Strugarek, E. Sonnendrücker, D. Zarzoso, Comput. Phys. Communications, 207 (2016) 35

[Hariri 2013] F. Hariri, M. Ottaviani, Computer Physics Communications 184 (2013) 2419

[Idomura 2016] Y. Idomura. A new hybrid kinetic electron model for full-f gyrokinetic simulations. J. Computational Physics, 313 (2016) 511

[ITER 1999] ITER Physics Expert Group on Confinement and Transport, ITER Physics Basis – Chapter 2: Plasma confinement and transport, Nucl. Fusion 39 (1999) 2175

[Lai 2001] M.-Ch., Lai, Numerical Methods for PDE (2001), Vol 17, Issue 3

[Lin 2002] Z. Lin, S. Ethier, T. S. Hahm, and W. M. Tang, Phys. Rev. Lett. 88 (2002) 195004

[McMillan 2010] McMillan B.F., Lapillonne X., Brunner S., Villard L., Jolliet S., Bottino A., Görler T. and Jenko F., 2010 Phys. Rev. Lett. 105 (2010) 155001

[Sarazin 1998] Y. Sarazin, Ph. Ghendrih, Phys. Plasmas 5 (1998) p.4214-4228

[Sarazin 2011] Y. Sarazin, V Grandgirard, J Abiteboul, S Allfrey, X Garbet, Ph Ghendrih, G Latu, A Strugarek, G Dif-Pradalier, P H Diamond, S Ku, C S Chang, B F McMillan, T M Tran, L Villard, S Jolliet, A Bottino, P Angelino, Nucl. Fusion 51 (2011) 103023

1.7. Publications and Presentations of GYSELA results involving EoCoE work

Publications in peer reviewed journals

[Bouzat, 2018] N. Bouzat, C. Bressan, V. Grandgirard, G. Latu, M. Mehrenberger, to appear in ESAIM Proceedings (2018) https://hal.archives-ouvertes.fr/hal-01653022

[Caschera 2018a] E. Caschera et al., “Immersed boundary testing in global, flux-driven, gyrokinetic simulations”, to appear in J. Phys. Conf. Series (2018)

[Caschera 2018b] E. Caschera et al., "Energy confinement time scaling from global and flux-driven gyrokinetic simulations”, in preparation, 2018

[Dif-Pradalier 2018a] G. Dif-Pradalier et al., “The ExB Staircase of Magnetised Plasmas”, Nucl. Fusion 57 (2017) 066026

[Dif-Pradalier 2018b] G. Dif-Pradalier et al., “Evidence for Global SOL-Edge-Core interplay in magnetised plasmas”, Plasma & Fusion Research: Rapid Commun. 12 (2017) 1203012

[Donnel, 2018a] Peter Donnel, Xavier Garbet; Yanick Sarazin; Virginie Grandgirard; Yuuichi Asahi; Nicolas Bouzat; Elisabetta Caschera; Guilhem Dif-Pradalier; Charles Ehrlacher; Philippe Ghendrih; Camille Gillot; Guillaume Latu; Chantal Passeron, “A multi-species collisional operator for full-F global gyrokinetics codes: Numerical aspects and validation with the GYSELA code”, to appear in Computer Physics Communications (2018)

[Donnel, 2018b]	P. Donnel, X. Garbet, Y. Sarazin, V. Grandgirard, N. Bouzat, E.Caschera, G. Dif-Pradalier, P. Ghendrih, C. Gillot, G. Latu, C. Passeron, "Neoclassical impurity flux in presence of turbulent generated poloidal asymmetries", to appear in J. Phys. Conf. Series (2018)
[Garbet 2018]	C. Ehrlacher, X. Garbet, V. Grandgirard, Y. Sarazin, P. Donnel, E. Caschera, P. Ghendrih, D. Zarzoso, "Contribution of trapped electrons to GAM damping", to appear in J. Phys. Conf. Series (2018)
[Ghendrih 2018]	Ph. Ghendrih et al., "Generation and dynamics of SOL corrugated profiles", to appear in J. Phys. Conf. Series (2018)
[Latu, 2018a]	G. Latu, M. Mehrenberger, Y Güçlü, M. Ottaviani, E. Sonnendrücker, Journal of Sci. Comp. (2018), Volume 74, Issue 3, pp 1601–1650
[Latu, 2018b]	G. Latu, Contribution to high-performance simulation and highly scalable numerical schemes, HDR diploma, University of Strasbourg, May 2018. http://icps.u-strasbg.fr/people/latu/public_html/docs/hdr_latu.pdf

International conferences and workshops:

E. Caschera et al.	"Immersed boundary testing in global, flux-driven, gyrokinetic simulations", Varenna conference, 2018, poster
E. Caschera et al.	"Energy Confinement Time Scaling law in GYSELA", Numerical Methods for the Kinetic Equations of Plasma Physics (NumKin), Garching, Germany (2017), oral
G. Dif-Pradalier et al.	"What is singular in flux-driven physics?", 20th ITPA meeting, Daejeon, Korea, 2018, oral
G. Dif-Pradalier et al.	"Poloidal Flows, Asymmetries and Multiscale Organisation in Interplaying Core-edge-SOL Turbulent Plasmas", 27th IAEA Fusion Energy Conference, Ahmedabad, India, 2018, poster
G. Dif-Pradalier et al.	"Near-Marginal Core & Edge Turbulent Organisation", 8th Asia-Pacific Transport Working Group (APTWG2018) International Conference, Leshan, China, oral
P. Donnel et al.	"Synergy between neoclassical and turbulent impurity transport: Role and origin of poloidal asymmetries", Joint Varenna-Lausanne international workshop on the Theory of Fusion Plasmas, 2018, oral
X. Garbet et al.	"Contribution of trapped electrons to GAM damping", Joint Varenna-Lausanne international workshop on the Theory of Fusion Plasmas, 2018, poster
Ph. Ghendrih et al.	"Generation and dynamics of SOL corrugated profiles", Joint Varenna-Lausanne international workshop on the Theory of Fusion Plasmas, 2018, poster
Ph. Ghendrih et al.	"PoPe verification & model reduction, application: 1D-1V multispecies kinetics GYSELA confinement time" Numerical Methods for the Kinetic Equations of Plasma Physics (NumKin), Garching, Germany (2017), oral
Y. Sarazin et al.	"HPC modelling of turbulent transport in tokamak plasmas: main results & critical physical issues", General conference of the French Physical Society, Plasma Physics Division, Bordeaux (France), June 12-14, 2018, oral
Y. Sarazin et al.	"Non-local features of flux driven gyrokinetic simulations", Joint EU-US Transport Task Force workshop, Sevilla (Spain), 2018, poster
Y. Sarazin et al.	"Impact of SOL-like boundary on flux driven gyrokinetic simulations", Joint EU-US Transport Task Force workshop, Sevilla (Spain), 2018, oral

2. Progress in nonlinear MHD modeling of Edge Localized Modes (ELMs) and ELMs control by Resonant Magnetic Perturbations (RPMs) using code JOREK

2.1. Introduction

The aim of the ITER project is the demonstration of the scientific feasibility of a nuclear fusion reactor based on a magnetic confinement concept as a future source of energy [1-2]. The large increase of the plasma energy with the size of the machine leads to large steady-state heat fluxes on plasma facing components (PFC). The ITER divertor is designed to handle these large stationary heat fluxes up to ~10MW/m^2 [1-2]. However, magneto-hydro-dynamic (MHD) instabilities in tokamak plasmas can lead to transient bursts of heat fluxes of much larger amplitude than the steady-state fluxes. Edge Localised Modes (ELMs), driven by the pressure gradient and/or the current flowing in the plasma, are typical for the high confinement (H-mode) scenario in tokamaks [3]. ELMs generate a perturbation of the structure of the magnetic field leading to quasi-periodic transient energy losses on a few hundred microseconds time scale [4]. Each ELM can release up to 10-20% of the thermal plasma energy [2] which, when scaled to ITER, represent 10-20MJ and would result in transient large heat fluxes of several GW/m^2, leading to an enhanced erosion of PFC and potentially representing an issue for the ITER divertor lifetime [1-2]. This means that ELMs in ITER need to be controlled, either mitigated by limiting their amplitude or by completely stabilizing the ELM instability. At present, the intensive experimental and theoretical study of ELMs physics is particularly oriented towards finding and optimizing the methods of ELMs control which can be used in ITER [1]. The application of Resonant Magnetic Perturbations (RMPs) demonstrated the possibility of total Edge Localized Modes (ELMs) suppression or strong mitigation of their size [2-10] motivating the use of this method in ITER. The non-linear MHD theory and modeling made significant progress to refine the understanding of the RMP interaction with the plasma [16-22]. In particular, it was demonstrated that RMPs penetration in the plasma is conditioned by the rotating plasma response [18,22]. The generation of current perturbations on the rational surfaces in plasma can prevent magnetic reconnections, leading to the screening of RMPs. Note that at some plasma parameters, RMPs can, on the contrary, be amplified [18,19]. Moreover RMPs are only the one source of the 3D magnetic perturbations in the existing tokamaks and ITER. In particular for ITER 3D boundary in magnetic topology will be due to the presence of Test Blanket Modules(TBMs), inhomogeneous toroidal field so-called toroidal ripples (TR) and the presence of ferritic inserts to correct them (FI). [23]. Similar to RMPs all 3D fields in plasma can be different from vacuum modelling and hence plasma response should be taken into account.

In the present project EoCoE-1 we did significant progress in understanding of ELMs dynamics and in particular non-linear crash phase and cycling regimes, physics of plasma response to 3D fields and interaction of ELMs with RMPs using non-linear resistive MHD code JOREK [24] in realistic tokamak geometry, including X-point, Scrape-Off Layer (SOL) and divertor. For this purpose the JOREK code was further developed in this project [25,26,27] to include relevant physics: a toroidal rotation source, neoclassical poloidal viscosity (to describe poloidal rotation dynamics) and two fluid diamagnetic effects, essential in the pedestal region with a strong pressure gradient.

The present report is organized as follows.

In the Section 2.2 we describe the main features of the model we used including the procedure of the construction of the adaptive grids which was the common subject for the developments in all pillars of EoCoE.
In the Section 2.3 we describe briefly the main achievements in understanding of ELM physics accomplished during EoCoE project. In particular ELM dynamics on linear and non-linear phase are described showing the essential role of the implemented into the model two fluid diamagnetic flows. Modelling for existing tokamaks JET (UK) and KSTAR (Korea) is presented followed by ITER parameters case in Sec.4. It was demonstrated that divertor heat fluxes paten is strongly influenced by drifts in confined plasma and in SOL resulting in agreement with experimental observations.
In Section 2.34 modelling of 3D fields (RMPs and TBMs,FI,TR for ITER case) and interaction of RMPs with ELMs are described. In particular the modelling results for AUG (Germany) and future ITER machine are presented.
Note that to reach ITER parameters was the main task of our part of EoCoE-1 project which was accomplished in many aspects.

2.2.JOREK model with flows and flux-aligned grid construction.

We used the non-linear resistive MHD code JOREK [24], with flows relevant for this study included in the model [18,25,26,27]. For the following discussion we recall the essential features which were included in the model. In particular toroidal plasma rotation and two fluid diamagnetic effects are essential in the pedestal region with a strong pressure gradient [18,25-27]. The normalized set of reduced MHD equations with two fluid diamagnetic and neoclassical effects solved here are presented in details in [18,27]. The boundary conditions around the computational domain correspond to those of an ideally conducting wall, where all perturbations are set to zero. On the divertor targets Bohm sheath boundary conditions were used for the fluid velocity and the heat flux normal to the target plates. The temperature and density have free outflow boundary conditions at the target.
The iso-parametric cubic Bezier finite elements were used to construct 2D grid in the poloidal cross-section on flux-aligned grid [28]. The continuity of all variables and their derivatives including coordinates (R, Z) is satisfied on this C-1 the grid. Flux aligned grid is practical and even more necessary in many applications in tokamak modelling and in particular in MHD to optimize numerical representation and solution of the problem. Firstly the MHD physics parallel and perpendicular to magnetic fields is very anisotropic. MHD modes are developing essentially in direction perpendicular to the magnetic flux surfaces and also heat conduction coefficient in parallel direction is much larger that perpendicular one: $K_{\parallel} / K_{\perp} = 10^{11} - 10^{8}$. The procedure of flux grid construction is following. JOREK includes a Grad-Shafranov (GS) solver which solves initial equilibrium without flows on the polar grid (Fig.1). The input needed for this step is magnetic poloidal flux at the boundary, pressure and current profiles and their derivatives which is usually calculated by EFIT or other static equilibrium codes.

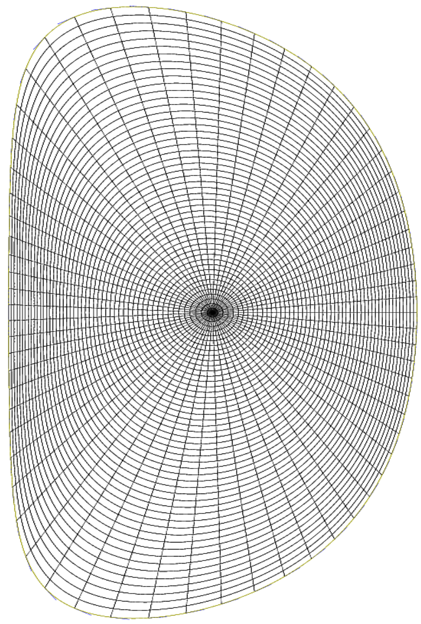	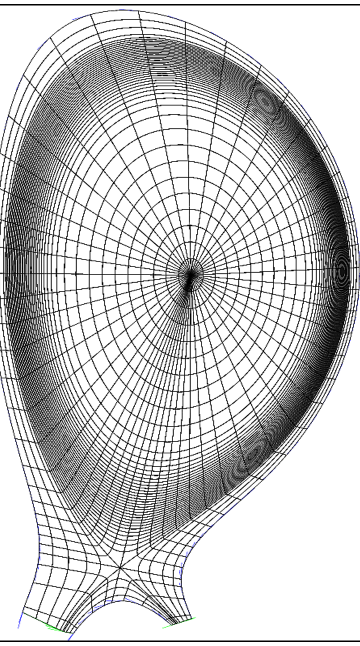	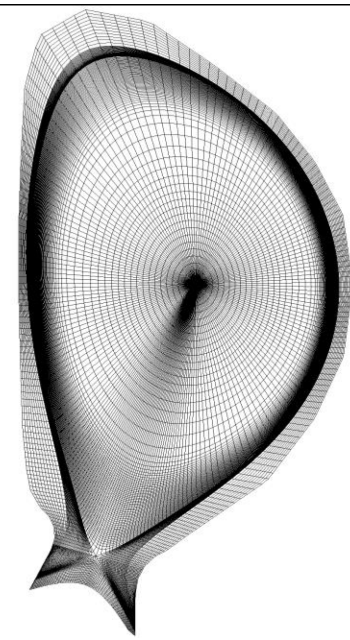
Fig.1. Polar grid in JOREK	*Fig.2 Flux aligned grid. JET case*	*Fig3. Flux aligned grid and extension to the realistic wall for ITER case.*

JOREK maps initial GS equilibrium to a flux surface aligned finite element grid including x-point and SOL. The finite element grid is aligned to equilibrium flux surfaces for the three regions of the core, the SOL and the private region (Fig.2). The boundary of the computational domain is limited by the flux surfaces and divertor target plates. Then equilibrium recalculated on aligned grid which is the starting points for non-linear MHD simulations or for calculation of the equilibrium with flows. There is an option to include realistic wall, so the grid is smoothly extended to the wall shape, this part of the grid is not flux-aligned (Fig.3).

The toroidal dimension is represented by a Fourier series. The time stepping is done using the implicit Crank-Nicolson scheme [27,28]. Resulting sparse system of equations is solved using a Generalized Minimal REsidual Solver (GMRES) with the preconditioner obtained by solving independently each sub-matrix corresponding to non-coupled Fourier harmonics. These sub-matrices are solved using the direct parallel sparse matrix solver PaStiX [29]. First the simulation starts on the initial flux-aligned mesh only for axisymmetric $n = 0$ component without other toroidal modes and continues until all flows (parallel and perpendicular) in the plasma core and SOL are established. Typical time to reach equilibrium with flows is about *~0.5-1 ms.* Then other harmonics are initialized at the noise level.

RMPs and other 3D fields (TBMS, FI, TR) were introduced in the code as follows. The magnetic perturbations generated by external coils were calculated by the vacuum ERGOS code [30] and are imposed as boundary conditions increasing in time on about ms time. The progressive switch on of RMPs on the boundary was implemented for numerical reasons to avoid transient un-physical currents at the edge in vacuum region. In the present model the magnetic flux, vorticity, mass density, temperature, current, electrostatic potential and parallel velocity self-consistently evolve, taking into account the plasma response to 3D fields including RMPs.

2.3. Modelling of ELMs dynamics

2.3.1. JET parameters

ELM simulations are performed for JET-like plasma parameters and geometry, at low triangularity shape, major radius $R_0 = 3$ m, minor radius a = 1 m, toroidal magnetic field $B_t = 2.9$ T and safety factor $q_{95} \sim 3$. Established H-mode experimental profiles are taken initially, with central electron density $n_{e,0} = 6.10^{19}$ m^{-3} and central temperature $T_{e,0} = 5$ keV. The pedestal density and temperature are $n_{e,ped} = 3.8 \times 10$^19 m−3 and $T_{e,ped} = 2.5$ keV. More details can be found in [26]. In this report we only briefly present summary of the main and totally new results obtained for the first time in this work.

In the modeling without diamagnetic drifts, the ELM crash is generated by the chosen initially unstable pressure profile. After the crash, the unstable modes remain unstable, and the residual magnetic activity expels the plasma outside the separatrix, which prevents the pedestal from building-up again. The example is given for the case of an n = 8 unstable toroidal mode. The ELM crash corresponds to a large peak of magnetic and kinetic energy (Fig.4). At the crash, the large magnetic activity leads to a strong ergodization of the edge. After the crash, magnetic islands remain at lower level for $\psi > 0.85$ and an ergodic layer subsists. The enhanced transport prevents the reconstruction of the pedestal profiles and keeps the plasma below the peeling-ballooning stability limit, thus a second ELM cannot be obtained in the simulations without diamagnetic effects [26].

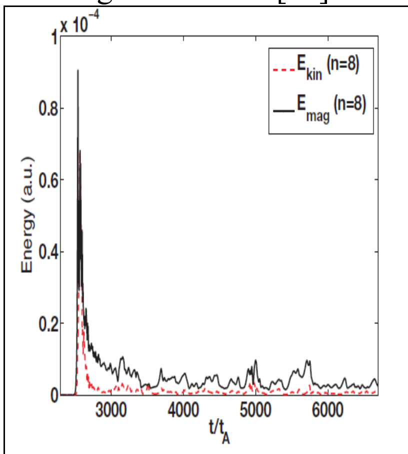

Fig.4 Time variation of the magnetic and kinetic energies of the mode n = 8 without diamagnetic effects.

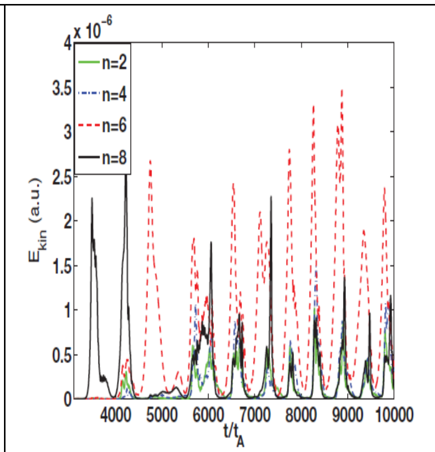

Fig.5. Kinetic energy of the modes n = 2–8 in the multiharmonic n = 0 : 2 : 8 simulation with diamagnetic effects.

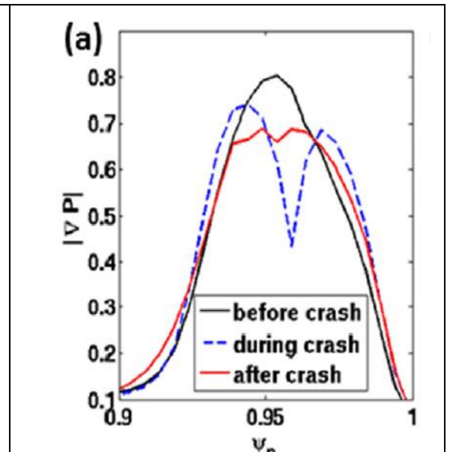

Fig.6. In quasi-periodic regime: (a) edge pressure gradient before, during and after an ELM.

Modelling of ELM with diamagnetic drifts enabled to simulate cycles of ELM crashes for the first time. The diamagnetic stabilization has two major effects on ELMs. First, it reduces the amplitude of the ELM perturbation and crash size (Compare Fig.4 and 5). After the first ELM crash, we observe the second major role of the diamagnetic stabilization: instead of remaining unstable after the crash, the plasma is stabilized by the diamagnetic rotation. Only when the pressure profile is built up by the applied heating power, the plasma is destabilized again. The ballooning modes are growing again until a threshold in pressure gradient is reached (Fig.6), triggering the second, third, etc. ELM relaxation.

Another important discovery was made in modelling with diamagnetic drifts. It concerns the pattern of divertor heat fluxes. is important to notice that this diamagnetic advection of the density makes that more density reaches the inner divertor plate than the outer plate, hence the heat flux reaching the divertor at the ion sound speed (Bohm boundary condition) is deposited near-symmetrically in the inner and outer divertor plates: even though the temperature is larger on the outer than on the inner side due to localization of ELM instability on LFS, the density is larger in the inner region so a similar power, proportional to both the plasma temperature and density, reaches the inner and outer divertor target plates due to an ELM. As an example, Fig.7(b) and (c) present the near-symmetric power deposition of the heat flux in the simulation of a realistic JET shot #77329, where the diamagnetic, neoclassical and toroidal flows have been taken into account. In comparison, in simulations made without flows (Fig.7(a) and (b)), the outer divertor received almost all the heat power. This was in contradiction with the experimental observations where the deposit is either symmetric on inner and outer divertor plates or two times larger in the inner divertor [31,32]. Thus our simulations with diamagnetic drifts allow for a more realistic reproduction of the ELM dynamics up to the deposition on the divertor.

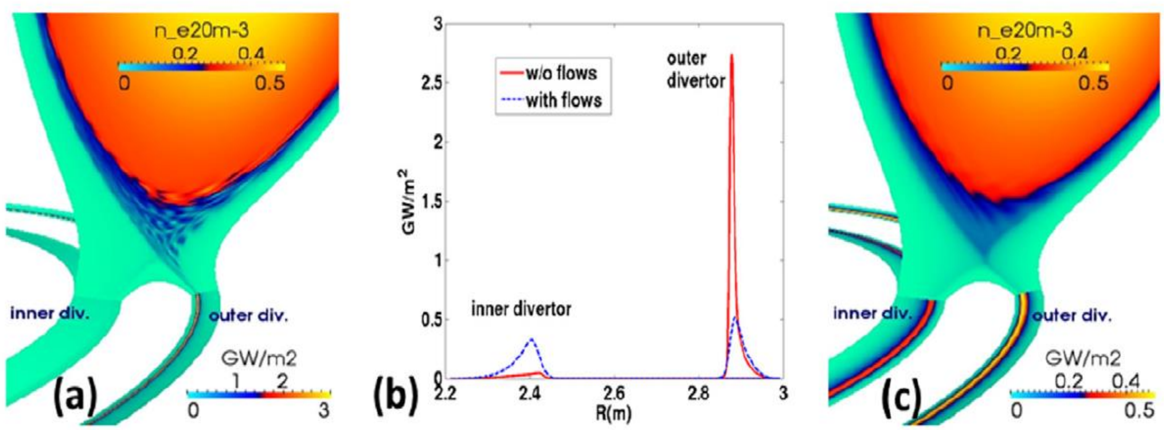

Fig.7. Heat flux (in MW/m2) reaching the inner and outer divertor target plates after an ELM: without flows (a) or with diamagnetic, neoclassical and toroidal flows (c). A radial section along the divertor is plotted in (b): almost all flux reaches the outer divertor (full line) without flows whereas the deposition is near-symmetric with flows (dash line).

2.3.2. KSTAR parameters

The very new result obtained in the period of the EoCoE project we would like to report here is the explanation of experimental observations on many machines and in particular on KSTAR (Korea)n about ELM dynamics. The non-linear MHD modelling of the full ELM crash dynamics was done using the JOREK code with two fluid diamagnetic and neoclassical effects for the KSTAR pulse #7328 parameters and compared to the ECEI diagnostic observations [27]. Most of the experimentally observed features were reproduced in JOREK modelling. In particular the structure and localization of the medium *n (n=5-8)* peeling-ballooning modes in the pedestal region inside the separatrix, poloidal rotation frequencies and the direction of the modes rotation before ELM crash are similar to the experimental observations (Fig.8-10). It was shown that the observed poloidal rotation of the modes in the inter-ELM periods far from the ELM crash is of the order of the $\sim \vec{E} \times \vec{B}$ velocity and can be in the electron diamagnetic direction (more common observation in many tokamaks) and in the ion diamagnetic direction at relatively large toroidal rotation, which was the case for the KSTAR pulse modeled. On the highly non-linear phase of ELM crash the regular rotation of the modes decreases and ELM filaments are expelled to the SOL. More ELM power is found in the inner divertor (in/out =2:1) compared to the outer divertor

(Fig.8) with two fluid diamagnetic and E×B drifts included in the model which is similar to the experimental findings and previous case for JET parameters. Multi-modes (*n=1-8*) modelling demonstrated the acceleration of the growth of all peeling-ballooning modes and the destabilization of the previously linearly stable modes while approaching the ELM crash. This is due to the strong non-linear coupling of the modes in this phase. In multi-ELMs regimes in the inter-ELM periods and before the ELM crash the temperature fluctuations spectrum in modelling is similar to the one observed in experiment. In particular the presence of several unstable modes *(n=5-8)* in the range of frequencies *(5-30kHz)* were obtained (Fig.11). The time duration of these coherent structures varies from *0.15ms* to *2ms* in modelling similar to experiment.

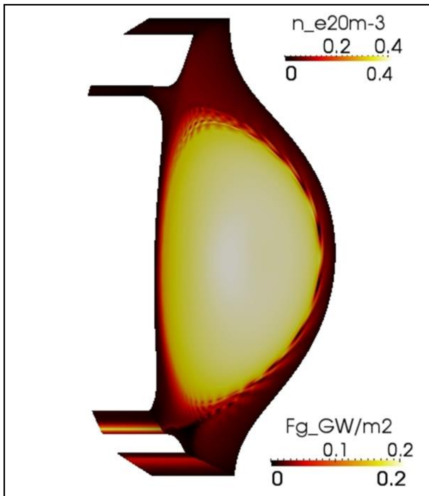

Fig.8. Density (upper scale in [10^20m-3]) filaments during non-linear phase of an ELM and maximum parallel heat flux (bottom scale in [GW/m2]) in the inner and outer divertor due to an ELM.

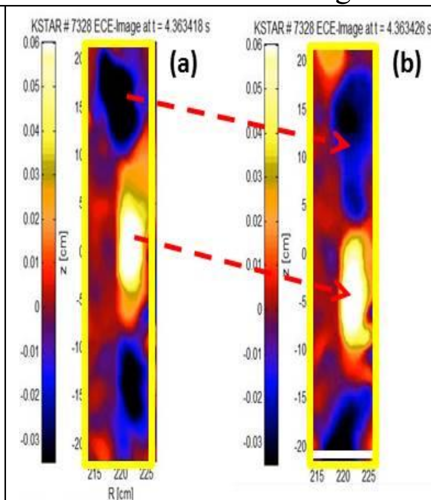

Fig.9. Two images of temperature fluctuations before ELM crash separated by ~0.008ms in time in non-linear MHD modelling in single harmonic n=8 simulation at Vtor =325km/s.

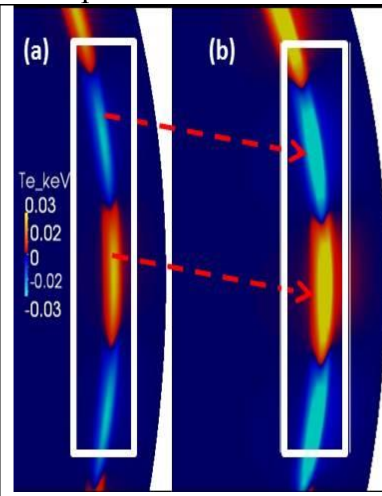

Fig.10. Two images of temperature fluctuations before ELM crash separated by ~0.008ms in time in non-linear MHD modelling in single harmonic n=8 simulation at Vtor =325km/s.

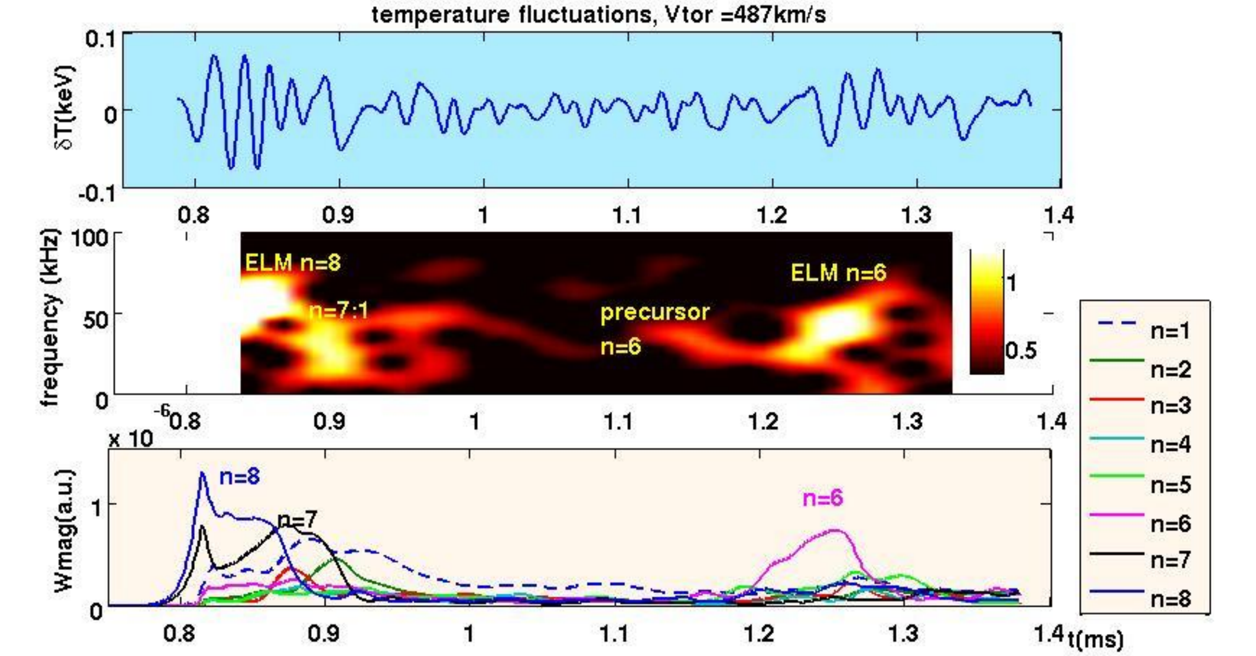

Fig.11. Temperature fluctuations in the pedestal at mid-plane in JOREK modelling (upper frame), frequency spectrum (middle) and evolution of the magnetic energy in time (bottom) for multi-harmonics simulation (n=1-8) of an ELM at increased Vtor=487km/s and 9MW NBI power.

2.4.ITER parameters. ELMs and ELMs control by RMPs

ITER modelling represent particular difficulties because of larger size and lower resistivity compared to JET, KASTAR cases. Firstly the natural ELM in ITER was modelled taking into account all relevant flows. Here we used the equilibrium and plasma parameters of the ITER standard H-mode scenario *15MA/5.3T*, *R=6.2m*, *a=2m*, $q_{95}=3.5$, central density $n_{e0} = 8.10^{19} m^{-3}$, temperature : $T_{e0} = 27.8 keV$ and the he initial central toroidal rotation profile is similar to the temperature profile with central rotation frequency *~1kHz*. Flux aligned grid near X-point with realistic representation of ITER divertor (points indicate its position), initial profiles, parallel Mach number (Mach=$V_{\|}/C_s$) are presented in (Fig.12-14).

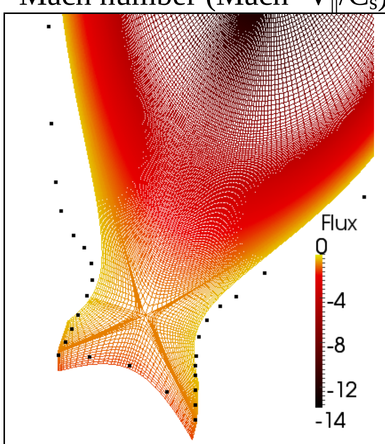

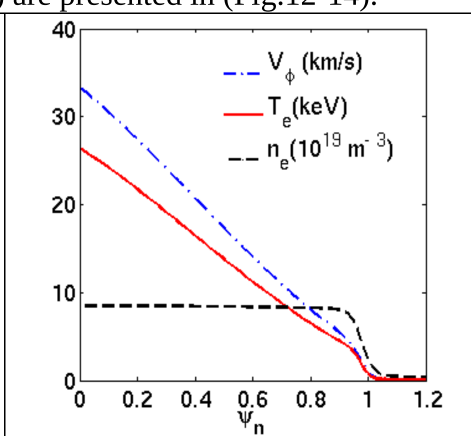

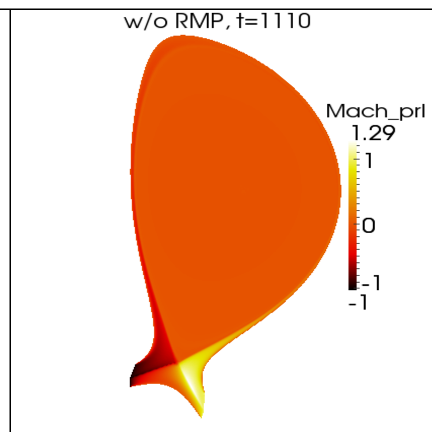

Fig.12. ITER equilibrium flux aligned mesh used in modeling.

Fig13. Plasma parameters used in modeling for ITER standard H-mode

Fig.14. Mach number for parallel flow in ITER equilibrium with all

Zoom near X-point.	*15MA/5.3T scenario.*	*flows included. Central toroidal rotation frequency ~1kHz.*

To study ELM mitigation by RMPs in ITER the comparison of the natural ELM and ELM with applied RMPs n=3 was done. In both cases toroidal modes n=3-9 were taken into account. Without RMPs the most unstable was n=9 mode and other modes n=3,6 were stable in the linear regime but are triggered on the non-linear stage due to the non-linear coupling (Fig.15 left, Fig.16).

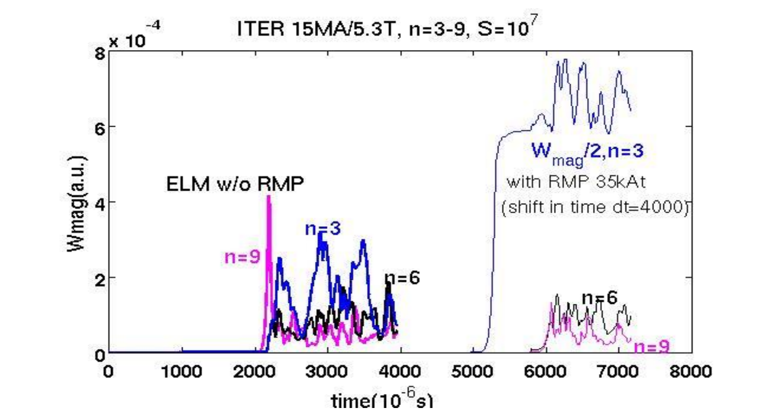

Fig.15. Magnetic energy on n=3:9 modes in unmitigated and mitigated by RMP (n=3,35kAt) ELM in ITER.

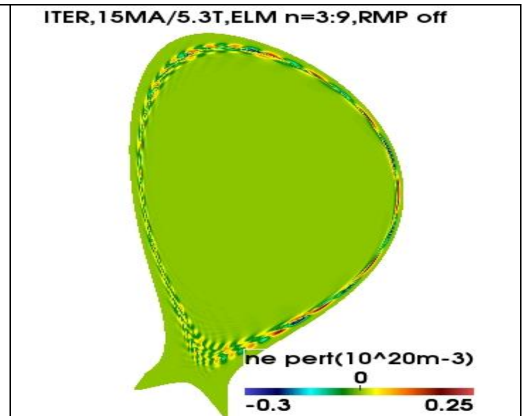

Fig.16. Density perturbation in natural ELM n=3-9 for ITER parametrs.

With RMPs on (which are introduced initially as vacuum perturbation flux n=3,35kAt in the coils at the boundary [18]) the mode n=3 from external coils is dominant, modes n=6,9 are reduced and represent continues MHD turbulence (Fig.15 right) similar to JET ELM mitigation case described in [22]. On Fig.17,18,19 the plasma density near X-point is presented for natural ELM crash, with RMP n=3 only and with mitigated by RMPs ELMs. One can see that mitigated ELMs increase density transport, but in continued way which permit to avoid large ELM crashes due to the medium n unstable modes (here n=9).

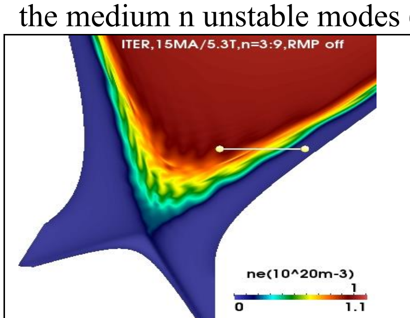

Fig.17. Density in ELM (n=3,6,9; most unstable mode was n=9) in ITERn (15MA/5.3T scenario)

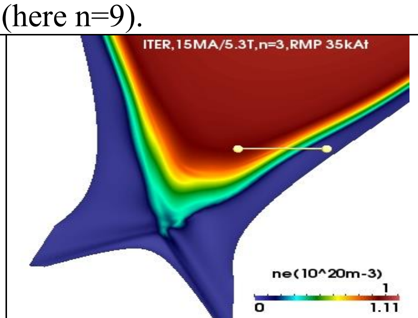

Fig.18. Density with RMP only (n=3,35kAt) in ITER

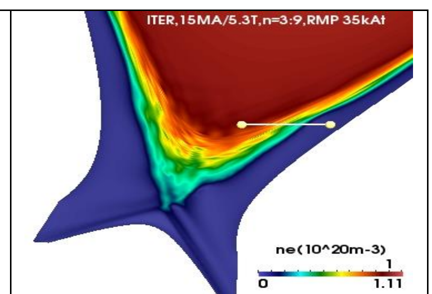

Fig.19. Density in mitigated by RMP (n=3, 35kAt) ELMs (n=3,6,9 modes were taken for modelling)

With RMPs the edge magnetic fluxes are destroyed and field lines became stochastic as it is shown in Fig.20-21.

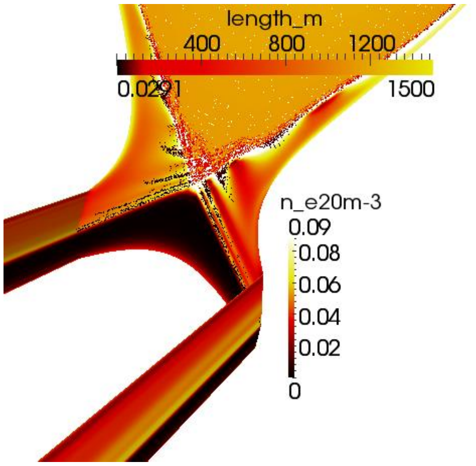

Fig.20. On the top: the connection lengths (Poincare plot) for the magnetic lines with starting points inside the initial separatrix near X-point. Bottom plot: Density on the divertor target plates with RMPs. Note splitting of the density paten near strike point in the divertor on the Low Field Side (bottom right).

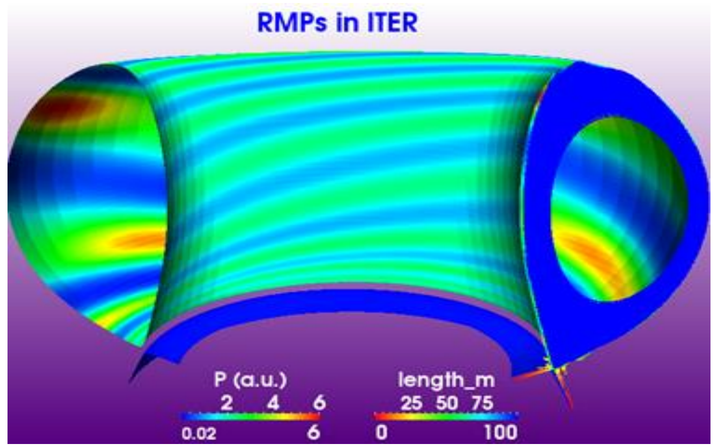

Fig.21. 3D structures of pressure on the initial (w/o RMPs) separatrix. The connection lengths (Poincare plot) for the magnetic lines with starting points inside the initial separatrix are presented on the right. Note characteristic "lobes" near X-point.

Important recent part of the JOREK modelling in ITER was estimation of 3D SOL and divertor heat and particle fluxes taking into account plasma response not only to RMP coils (Fig.22) but other sources of 3D fields like Test Blanket Modules(TBMs), inhomogeneous toroidal field so-called toroidal ripples (TR) and the presence of ferritic inserts to correct them (FI) [23] (Fig.23)

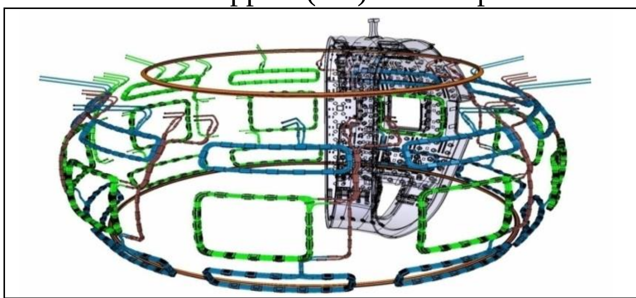

Fig.22. RMP coils in ITER

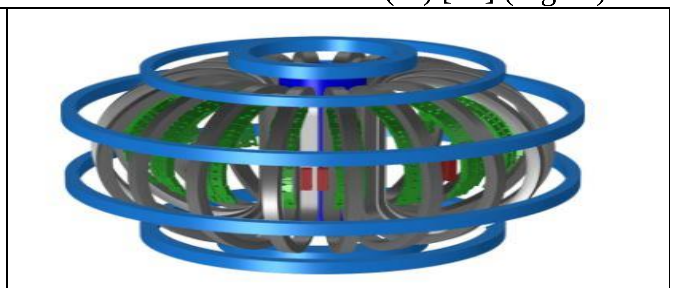

Fig.23. 18 TF coils –in gray; FI(in green),TBM in red

Edge ergodisation increases with RMP coils current and decreases with RMP main toroidal harmonic number at the same coil current. Largest for N=3(90kAt) (Fig.24)

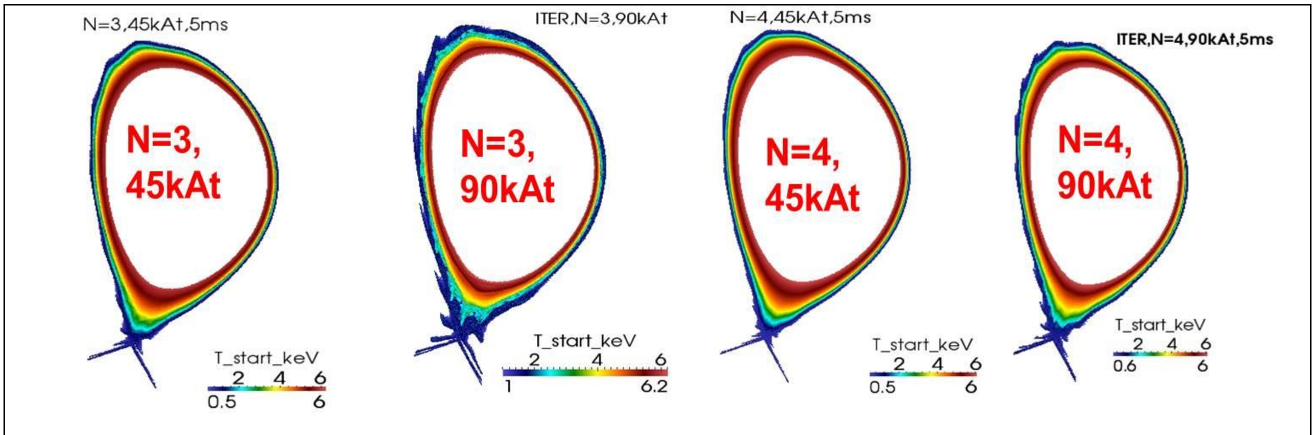

Fig.24. Magnetic topology at the boundary with RMPs in ITER

Normalised to the total power heat flux in inner and outer divertor is presented in Fig.25 for different spectrum of RMP. The main concern for divertor fluxes with RMPs that they are not axisymmetric toroidally, which lead potentially to increased erosion of materials. To uniform divertor fluxes the slow (~1Hz) rotation of RMPs was proposed, but it applies stresses on RMP coils since coils current amplitude should be changed up to 180kAt in each coil. To avoid stresses on coils but improve axisymmetry of heat flux compared to n=3 90kAt case (Fig.25) we proposed to use higher toroidal number in RMP spectrum (like n=4-Fig.26) or mixture of harmonics (n=3,4-Fig.27). These results were presented on ITPA (International Tokamak Physics Activity) meetings and to the particular attention of the ITER physics team. The characterization of magnetic topology of 3D SOL with RMP coils, TBMs, FI taking into account plasma response was done during the project. These data were given to the particle code ASCOT to estimate fast particle losses (alphas, NBI) due to 3D fields. The results in details are presented in our recent common paper [23]. RMPs with TBMs, FI, include main harmonics n=1:6 and produce slightly larger edge ergodisation and extension of divertor footprints compared to RMPs only (Fig.28-30). Non-linear coupling of modes with RMPs n=3 increases amplitude of n=6 harmonic. Note that only resonant harmonics are screened near rational surfaces [18]. Alpha particles and neutral beam ions losses (NBI) are estimated using ASCOT code with and without plasma response calculated by JOREK code. Alphas particle losses in vacuum 3D fields were 2MW, and with screening by rotating plasma:1.3MW, while NBI losses in vacuum: 1.2MW, and with plasma response-0.9MW. This is because screening of 3D fields by plasma rotation. In this report we presented only brief summary of the accomplished work and results. More can be find in the papers published in the period of the EoCoE project (see the list in Appendix)

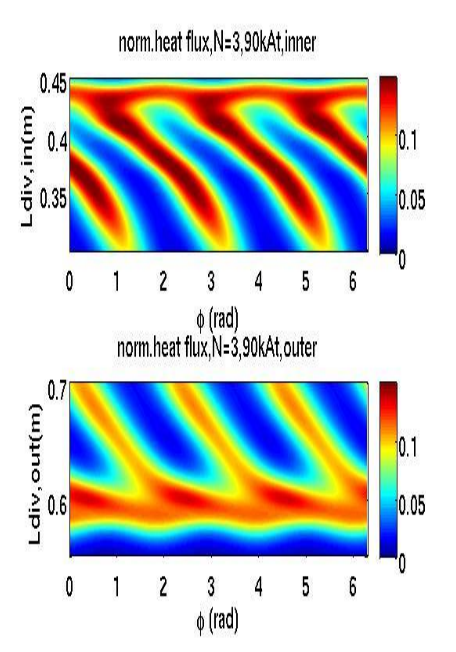	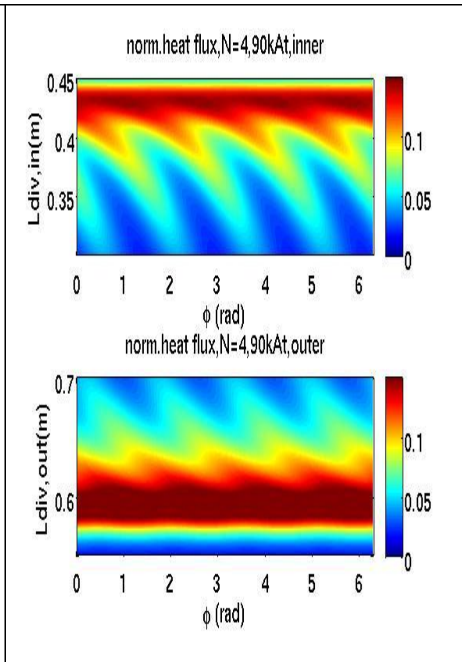	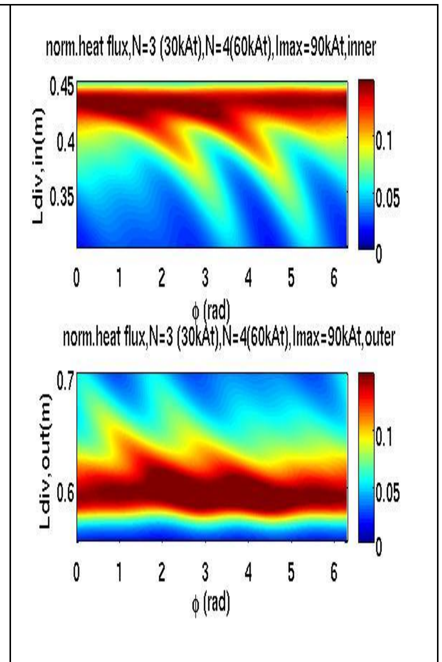
Fig.25. Divertor heat flux with RMP 90kAt,n=3 in ITER.	*Fig.26. Divertor heat flux with RMP 90kAt,n=4.*	*Fig.27. Divertor heat flux with mixture of harmonics RMP 60kAt,n=4 and 30kAt,n=3*

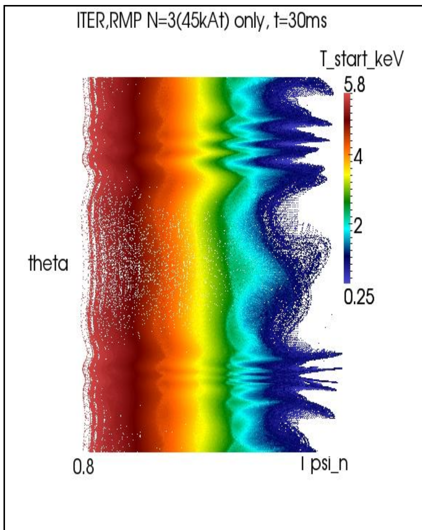	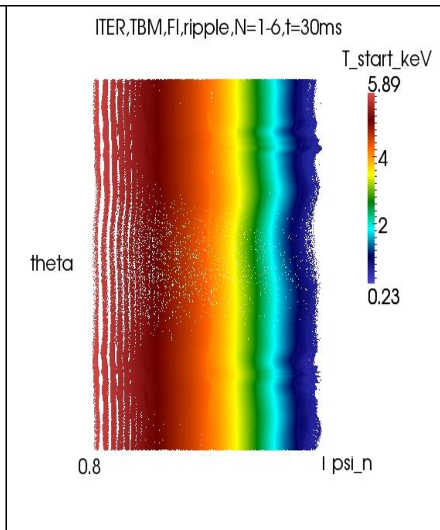	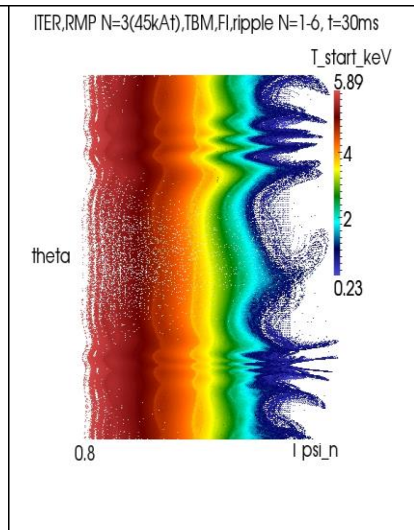
Fig.28	*Fig.29*	*Fig.30*

2.5.References

[1] Progress in the ITER Physics Basis Nucl Fusion 47 (2007)
[2] A Loarte A et al Nucl Fusion 54 033007(2014)
[3] M Becoulet et al Plasma Phys Control Fusion 45(2003) A93–A113
[4] T Eich et al Journal of Nuclear Materials 337–339 (2005) 669–676
[5] M Fenstermacher et al Phys. Plasmas 15 056122 (2008)

[6] T Evans et al Phys Rev Lett 92(2004) 235003(2004)
[7] Y Liang et al Phys Rev Lett 98 265004 (2007)
[8] J M Canik et al Nucl Fusion 50 034012 (2010)
[9] W Suttrop et al Phys Rev Lett 106 225004(2011)
[10] Y M Jeon et al Phys Rev Lett 109 035004(2012)
[11] A Kirk et al Phys Rev Lett 108 255003(2012)
[12] Y Sun et al Phys Rev Lett 117 115001 (2016)
[13] M J Schaffer et al Nucl. Fusion 48 (2008) 024004
[14] T Evans et al Nucl. Fusion 53 (2013) 093029(13p)
[15] R Fitzpatrick Phys Plasmas 5 3325(1998)
[16] H Strauss et al Nucl. Fusion 49, 055025 (2009)
[17] M Becoulet et al Nucl Fusion 52, 054003 (2012)
[18] F Orain et al Phys. Plasmas 20 102510 (2013).
[19] N Ferraro et al Nucl. Fusion 53, 073042 (2013).
[20] F L Waelbroeck et al Nucl Fusion 52 074004 (2012)
[21] Y Q Liu, R Akers et al Nucl Fusion 55(2015)063027(14pp)
[22] M Becoulet et al Phys Rev Lett 113(2014) 115001
[23] K Sarkimaki, J. Varje, M. Becoulet et al Nuclear Fusion 58(2018) 076021
[24] G T A Huysmans et al Nucl. Fusion 47 (2007) 659
[25]F Orain et al Phys Rev Letters 114, 035001 (2015)
[26]F Orain et al Plasma Phys. Control. Fusion 57 (2015) 014020 (10pp)
[27] M Becoulet et al Nuclear Fusion 57(2017)116059(12pp)
[28] O Czarny et al. J.Comp.Phys. 227, 2008.
[29] P. Henon et al. Parallel Comp. 34 345-362, 2008.
[30] M Becoulet Nucl Fusion 48 (2008) 024003
[31] Pitts R A et al 2007 Nucl. Fusion 47 1437
[32] Eich T, Herrmann A and Neuhauser J 2003 Phys. Rev. Lett. 91 195003
[33] O Schmitz et al Nucl. Fusion 56 (2016) 066008 (22pp)

2.6.JOREK publications on ELMs and their control by RMPs (2015-2018)

1)Mechanics of ELM control coil induced fast particle transport in ITER
By: Sarkimaki, Konsta; Varje, Jari; Becoulet, Marina; et al.
NUCLEAR FUSION Volume: 58 Issue: 7 Article Number: 076021 Published: JUL 2018
2)Nonlinear coupling induced toroidal structure of edge localized modes
By: Mink, A. F.; Hoelzl, M.; Wolfrum, E.; et al. Group Author(s): ASDEX Upgrade Team
NUCLEAR FUSION Volume: 58 Issue: 2 Article Number: 026011 Published: FEB 2018
3)Nonlinear MHD simulations of QH-mode DIII-D plasmas and implications for ITER high Q scenarios.
By: Liu, F.; Huijsmans, G. T. A.; Loarte, A.; et al.
PLASMA PHYSICS AND CONTROLLED FUSION Volume: 60 Issue: 1 Article Number: 014039 Published: JAN 2018
4) Non-linear MHD modelling of edge localized modes dynamics in KSTAR
By: Becoulet, M.; Kim, M.; Yun, G.; et al. NUCLEAR FUSION Volume: 57 Issue: 11 Article Number: 116059 Published: NOV 2017
5)Recent progress in the quantitative validation of JOREK simulations of ELMs in JET
By: Pamela, S. J. P.; Huijsmans, G. T. A.; Eich, T.; et al. Group Author(s): JET Contributors NUCLEAR FUSION Volume: 57 Issue: 7 Article Number: 076006 Published: JUL 2017
6)Non-linear modeling of the plasma response to RMPs in ASDEX Upgrade
By: Orain, F.; Hoelzl, M.; Viezzer, E.; et al.
Group Author(s): ASDEX Upgrade Team; EUROfusion MST1 Team

NUCLEAR FUSION Volume: 57 Issue: 2 Special Issue: SI Article Number: 022013 Published: FEB 2017
7)Three-dimensional modeling of plasma edge transport and divertor fluxes during application of resonant magnetic perturbations on ITER By: Schmitz, O.; Becoulet, M.; Cahyna, P.; et al. NUCLEAR FUSION Volume: 56 Issue: 6 Article Number: 066008 Published: JUN 2016
8)Edge localized mode rotation and the nonlinear dynamics of filaments
By: Morales, J. A.; Becoulet, M.; Garbet, X.; et al. PHYSICS OF PLASMAS Volume: 23 Issue: 4 Article Number: 042513 Published: APR 2016
9)Non-linear MHD simulations of ELMs in JET and quantitative comparisons to experiments By: Pamela, S.; Eich, T.; Frassinetti, L.; et al. Group Author(s): JET Contributors PLASMA PHYSICS AND CONTROLLED FUSION Volume: 58 Issue: 1 Special Issue: SI Article Number: 014026 Published: JAN 2016
10)Three-dimensional non-linear magnetohydrodynamic modeling of massive gas injection triggered disruptions in JET By: Fil, A.; Nardon, E.; Hoelzl, M.; et al. Group Author(s): JET Contributors PHYSICS OF PLASMAS Volume: 22 Issue: 6 Article Number: 062509 Published: JUN 2015
11).WEST Physics Basis By: Bourdelle, C.; Artaud, J. F.; Basiuk, V.; et al.
Group Author(s): JET Contributors NUCLEAR FUSION Volume: 55 Issue: 6 Article Number: 063017 Published: JUN 2015
12) Resistive Reduced MHD Modeling of Multi-Edge-Localized-Mode Cycles in Tokamak X-Point Plasmas By: Orain, F.; Becoulet, M.; Huijsmans, G. T. A.; et al. PHYSICAL REVIEW LETTERS Volume: 114 Issue: 3 Article Number: 035001 Published: JAN 22 2015
13)Non-linear MHD modeling of edge localized mode cycles and mitigation by resonant magnetic perturbations By: Orain, Francois; Becoulet, M.; Morales, J.; et al.
Conference: 41st European-Physical-Society Conference on Plasma Physics Location: Max Planck Inst Plasma Phys, Berlin, GERMANY Date: JUN 23-27, 2014 PLASMA PHYSICS AND CONTROLLED FUSION Volume: 57 Issue: 1 Article Number: 014020 Published: JAN 2015

3. Progress in edge turbulence and transport modelling using the TOKAM3X code

3.1.Introduction

The success of fusion experiments in ITER will be conditioned by our capability to both ensure the quality of plasma confinement, and to control the heat and particle fluxes on the walls of the machine. During the operation, the design of the magnetic configuration and of the shape of the walls as well as the tuning of the edge plasma conditions will be critical in order to satisfy conflicting constraints on the plasma scenario. On the one hand, fusion ignition requires the plasma to be sufficiently heated, fuelled and confined, and on the other hand, particle and heat handling on the tokamak wall require steady state exhaust without undue damage to the reactor itself, specifically its Plasma Facing Components (PFCs). These critical issues are largely dependent on the physics taking place in the peripheral region of the plasma, especially that of turbulent transport.

Concerning plasma confinement, ITER is designed to run in a specific regime, the so-called "H-mode" (High-confinement mode), characterized by a strong increase of the energy confinement compared with the standard "L-mode" (Low-confinement mode). The existence of H-mode has been demonstrated on all tokamaks equipped with a divertor beyond some threshold on the heating power applied to the plasma. Its realization in ITER is critical for the achievement of ITER's target of an energy amplification factor Q of 10. However, in spite of its discovery more than 30 years ago, H-mode still eludes the fusion community's understanding [Wagner, PPCF2007]. Experiments as well as reduced models have demonstrated that the bifurcation to this regime is related to a local drop of turbulent transport most probably due to the interaction between plasma micro-scale fluctuations and large scale sheared flows in the edge plasma, but the modelling of H-mode in self-consistent models (ie, not requiring ad-hoc parameters or terms) has not been obtained to date. There are clear indications that the magnetic configuration and plasma conditions in the edge plasma are key parameters impacting the transition to H-mode. In particular, the presence of an X-point in the edge magnetic equilibrium is a quasi-sine-qua-non condition to obtain H-mode.

Concerning heat and particle exhaust, in ITER the ratio between the power remaining to be extracted onto these PFCs and the power handling capability by state of the art technology for divertor PFCs is expected to be around 10 [Loarte, NF2007]. Consequently, optimized scenarios for ITER divertor operation will have to remove the bulk of the energy in the diverted plasma channel (and not in the core) before it contacts the divertor target plates. These optimized divertor operations and predictions on the wall power load remain uncertain, largely owing to an incomplete understanding of the mechanisms at play. Turbulent transport, determining the width of the heat flux foot-print on the target plates, and atomic and molecular physics related to the interaction of the plasma with the dense population of neutral particles, responsible for most of the dissipation of the plasma energy flux before it reaches the wall, are the main identified players in this phenomenology.

For both issues (H-mode confinement and plasma exhaust), the difficulty to generate a global description based on experimental measurements in tokamaks requires performing numerical simulations. From the current state of the art of the understanding, several key physics ingredients emerge that need to be included in the model to obtain consistent answers on these issues in sight of ITER. The numerical model should in particular include a self-consistent description of:

- 3D turbulent transverse transport of both particles and energy
- boundary conditions imposed by plasma-wall interactions
- the magnetic geometry in the edge plasma, especially the presence of an X-point in divertor configuration
- neutral particle recycling and its impact on the plasma particle and energy sources and sinks

Strong international effort has been invested for the last decade towards achieving these goals.

The 3D fluid turbulence code TOKAM3X is currently co-developed at CEA IRFM and Aix-Marseille University, in that frame. The fluid approach adopted in the project takes advantage of the relatively high collisionality of the edge plasma (mainly due to it relatively low temperature), thus allowing the use of collisional closures. Although this choice dramatically reduces the computing power demand compared with a kinetic or gyro-kinetic approach, ITER relevant cases including all the above-mentioned physics remain an extremely challenging target. A step-by-step approach is necessary to progress towards it.

At the time of launch of the EoCoE project, the TOKAM3X code had demonstrated its capability to model 3D turbulent particle transport in the edge plasma in an ideal circular concentric magnetic geometry [Tamain, CPP2014; Tamain, PPCF2015; Colin, JNM2015]. Heat transport was not treated at the time since the equations solved by the code relied on an isothermal assumption for the plasma. In the course of the EoCoE project, several key physics milestones have been achieved:

- the code's geometrical capabilities have been extended to arbitrary axisymmetric magnetic equilibria, allowing the modelling of turbulent transport in realistic divertor (X-point) geometry
- the isothermal assumption was relaxed by adding energy balance equations in the model, allowing the modelling of heat turbulent transport
- the TOKAM3X code has been coupled to the EIRENE kinetic neutrals codes, allowing the modelling of neutrals particles physics and their interaction with the plasma

We hereafter detail these 3 axes of progress.

3.2. Turbulence simulations in divertor geometry

The TOKAM3X code has from scratch been developed with special care given to being flexible in terms of magnetic geometry. Nevertheless, at the start of the EoCoE project, only simulations in idealized toroidal limiter geometry had been run in production due to numerical discretization issues arising around the X-point in divertor geometry. Indeed, TOKAM3X's geometrical flexibility stems from the use of domain decomposition into subdomains isomorphically equivalent to slabs, allowing the use of a structured mesh in each of the sub-domains (see Figure 1). This does not put any restriction on the describable geometries but special care must be taken around X-points where the discretization of poloidal gradient becomes degenerate. A specific interpolation method was developed for that purpose and proved to capture accurately the local gradients while insuring the numerical stability of the code.

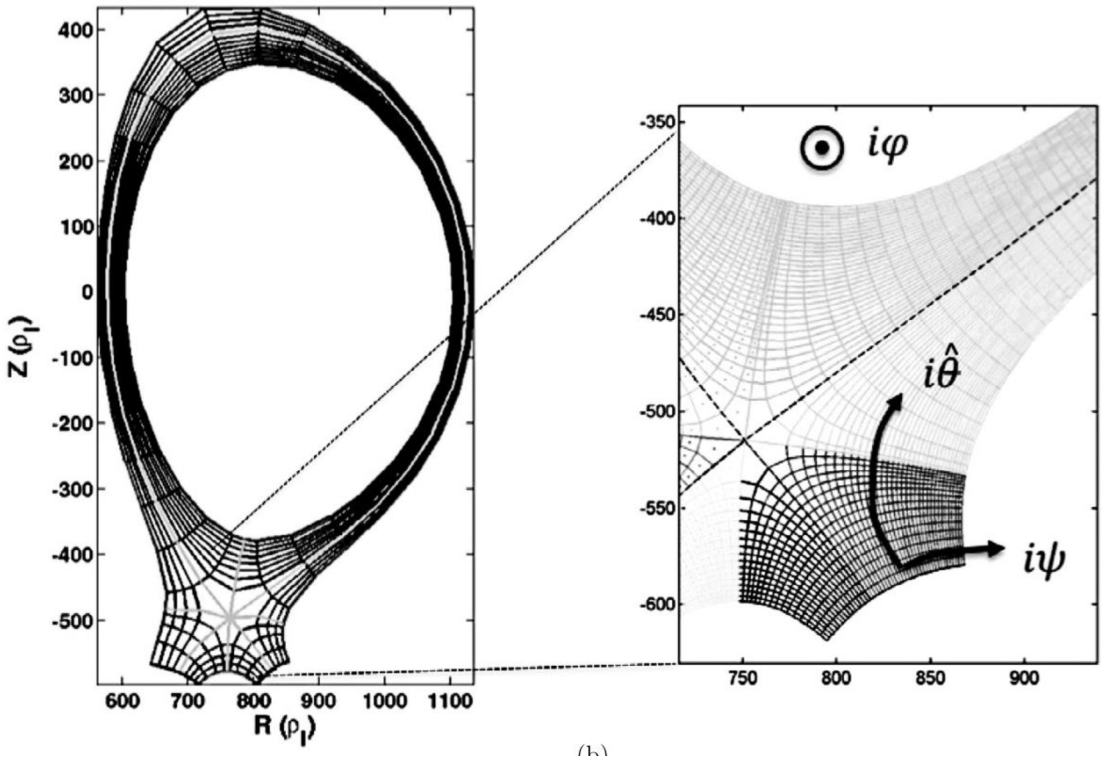

Figure 2: illustration of TOKAM3X poloidal mesh structure in diverted geometry (here for the JET tokamak). Left: global domain with only a few grid points plotted. Right: zoom on the divertor and X-point regions illustrating the domain decomposition into sub-regions discretized with a structured mesh. Figure extracted from [Tamain, JCP2016].

An example of the output of a TOKAM3X simulation in divertor geometry is given in Figure 2. These first simulations in a realistic COMPASS magnetic equilibrium allowed us to uncover key aspects of turbulent transport in diverted geometry. On the one hand, they demonstrated that, provided one takes into account correction factors related to the magnetic flux expansion, edge turbulence transport far from the X-point is largely similar to that observed in circular limited geometry, thus confirming the relevance of past TOKAM3X results [Galassi, NF2017; Galassi, PhD2017]. Nevertheless, several features specific to the divertor geometry were highlighted. The magnetic shear associated with the X-point was shown to damp turbulence and the associated transport in its vicinity as well as along the separatrix, leading to the development of a mild transport barrier. Turbulence was also shown to develop on the outboard side of the divertor region while the inner divertor leg remains quasi-quiescent. Diverted plasma simulations were also applied in support to experiments on the TCV tokamak. TOKAM3X simulations were able to recover experimental trends that could not be recovered in codes not solving turbulence in a 3D realistic diverted geometry. The complex distribution of turbulent transport in the divertor region was found as a key player in the response of heat loads at the targets as a function of the plasma geometry [Gallo, PPCF2018].

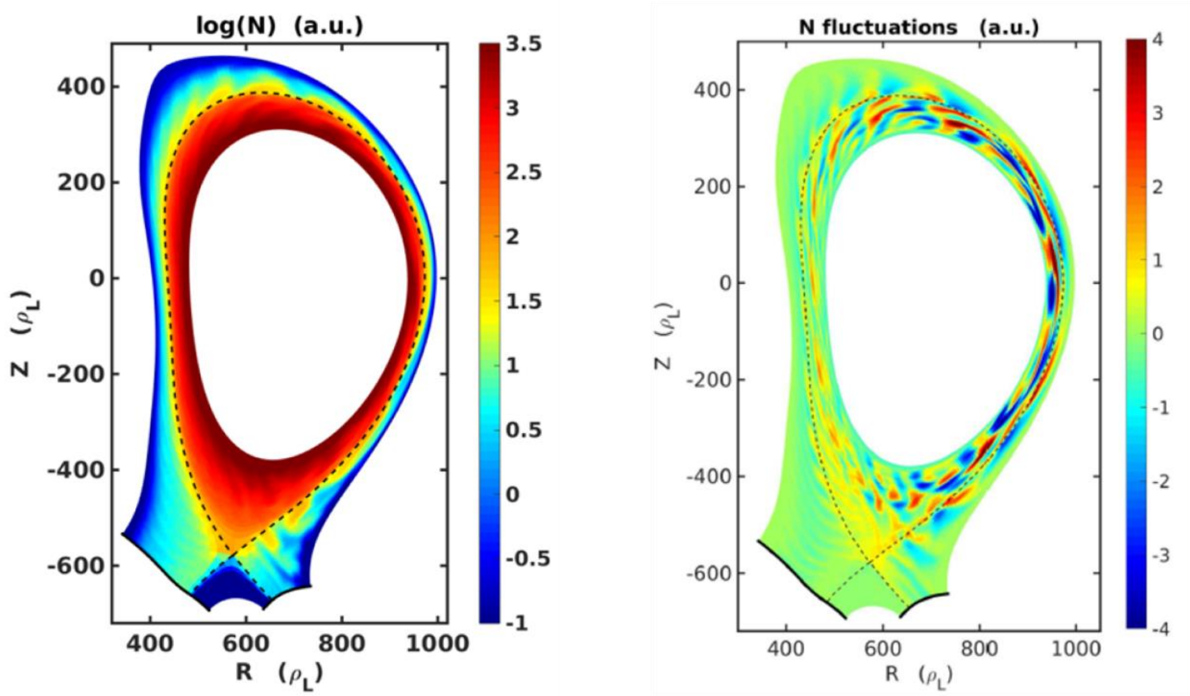

Figure 3: poloidal plane snapshots of the total density field (left, log scale) and its fluctuating part (right) in TOKAM3X turbulence simulations in diverted geometry. The magnetic equilibrium was here taken from experiments on the COMPASS tokamak. [Galassi, NF2017]

3.3. Heat turbulent transport

The development strategy of the TOKAM3X code consists in a step-wise enrichment of the physics model. At the start of the EoCoE project, TOKAM3X solved a simple 3D turbulence model based on an isothermal closure. The temperature fields of the 2 modelled species (electrons and ions) were considered frozen in time, thus reducing the number of partial differential equations to be solved down to 4 equations. The resulting model contained the key ingredients describing turbulent transport's dynamics, which allowed performing relevant studies on the basic properties of turbulence in the edge plasma of tokamaks. However, H-mode physics as well as heat exhaust are strongly dependent on transverse heat transport and demand a full non isothermal treatment to obtain a fully consistent picture of the physics at play. In particular, heat transport is strongly different from particle transport in the direction parallel to the magnetic field: while parallel particle transport is in essence solely convective, parallel heat transport can present a strong (often dominant) conductive component. Owing to the associated fast dynamics, solving the latter is challenging from a numerical point of view.

In the course of the EoCoE project, effort was invested in moving towards a non-isothermal model in TOKAM3X. 2 additional unknown fields (the electron and ion temperatures) were added with the 2 energy balance equations describing their time evolution. The fast dynamics associated with parallel heat conductions, especially for electrons, made necessary an implicit approach so as not to impact too dramatically the time step of the solver. In order to avoid a degradation of the parallel scalability, this required revisiting the domain decomposition across

MPI tasks to favour decomposition by flux surfaces and benefit from a natural parallelization of these terms. Another difficulty arose from the non-linear impact of temperature variations on boundary conditions, making it necessary to update at each time step the matrices of implicit linear systems. Taking advantage of the relatively slow time scale of evolution of plasma fields compared with the time step imposed by numerical stability considerations, we developed a so-called “short-cycling” scheme in which the linear solver matrices are updated at regular intervals but not at every time step.

Thanks to all these developments, the TOKAM3X code can now run non-isothermal turbulence simulations with fully consistent time and space evolution of temperature fields. First application cases were run in circular limited geometry for simplicity [Baudoin, CPP2018] (illustrated in Figure 3, left panel). It was found that at first order, the inclusion of temperature fluctuations does not change the main qualitative features of particle turbulent transport. Transverse fluxes remain dominated by strongly intermittent self-organized events, in the form of elongated filamentary structures as reported many times in experiments [Zweben, PPCF2007] and the resulting transport is strongly inhomogeneous and generates large scale parallel return flows [Asakura, JNM2007; Colin, JNM2015]. Heat transport follows the same pattern but a clear difference can be observed between the underlying mechanisms for electrons and ions. While ion energy transport is largely dominated by convection (i.e., heat being transported with particles), electron energy transport exhibits a non-negligible conductive contribution (i.e., heat being transported without an associated particle flux) whose weight is similar to convection in the Scrape-Off Layer (Figure 3, right panel). Such results shed new light on edge transverse energy transport in the frame of a recent controversy on the dominant mechanisms driving these fluxes [Goldston, NF2012]. Preliminary diverted cases have also been run successfully in the frame of simulations with neutral particles physics (see next section).

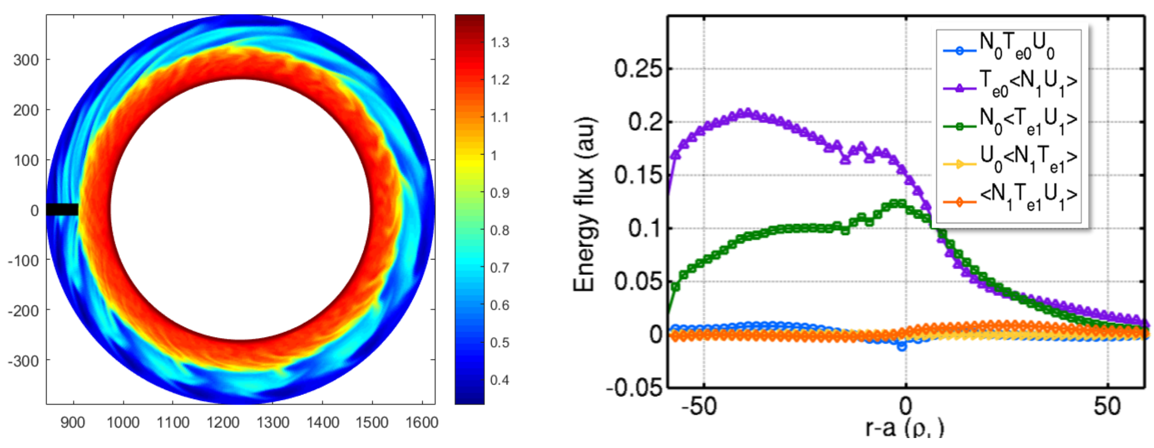

Figure 4: Left: snapshot of electron temperature field in a turbulent non-isothermal simulation in circular limited geometry. Right: radial profile of the radial electron energy flux decomposed in its various components. The convective (purple) and conductive (green) dominate throughout the profile.

3.4. Coupling to neutral particles physics

Neutral particles are a major player of edge plasma physics. When the plasma gets in contact with the solid wall of the reactor, as it is the case at the target plates in the divertor, the ions flowing out of the plasma instantly recombine with electrons from the wall to form neutral atoms or molecules. Owing to their absence of electric charge, these neutral particles are not sensitive to the confining magnetic field and the vast majority of them (more than 99%) flows back into the plasma where they end up being re-ionized or undergo complex chemical reactions. This circular flow of particles is called “recycling” and, in the usual divertor conditions encountered in medium or large tokamaks, it accounts for most of the particle source (e.g., more than 99% in ITER plasmas [Kukushkin, JNM2011]). Strong momentum and energy sinks are associated with this particle recycling which are key player in the divertor operation in order to dissipate particle and heat fluxes before they reach the targets.

Historically, neutral particles physics studies have been carried out almost exclusively in the frame of 2D transport modelling, i.e. 2D edge plasma models in which transverse turbulent transport is described by gradient-diffusion laws with prescribed ad-hoc diffusion coefficients. The vast majority of turbulent transport studies have been carried out without including or considering neutral particles physics. It was implicitly assumed that turbulent transport develops independently of the sources and sinks imposed by recycling neutrals in the divertor. However, the observation of an impact of divertor recycling conditions on edge plasma profiles away from the divertor sheds doubts on this assumption [Carallero, NF2014]. Moreover, in a frame where turbulence simulations are driven by an imposed particle (or energy) flux, it appears unlikely that the exact distribution of particle and energy sources / sinks in the edge plasma would not impact the turbulence phenomenology. In any case, if one has the ambition to use edge turbulence codes to predict quantitatively particle and heat fluxes to the target plates in ITER, a fully consistent modelling including both turbulent transport and neutral particles physics appears mandatory.

The inclusion of neutrals physics is one of the main outcomes of the EoCoE project concerning the TOKAM3X turbulence code. Owing to the large number of atomic and molecular reactions neutral particles can undergo and given the necessity of a kinetic approach due to the generally low collisionality of neutral particles, writing from scratch a dedicated neutral particles solver for TOKAM3X would have been a very complex task and was not considered. Instead, the choice was made to capitalize on the experience of 2D edge transport codes, especially the SOLEDGE2D code developed in Cadarache and Aix-Marseille University [Bufferand, NF2015] which was coupled like most of its competitors with the kinetic neutrals Monte-Carlo code EIRENE. Thus, TOKAM3X was coupled to EIRENE using the same interface STYX as was used for SOLEDGE2D [Fan, CPP2018]. Note that the extension of TOKAM3X to a non-isothermal model (see previous section) was a mandatory preliminary task before including neutrals physics, as temperature variations play a key role in the phenomenology related to recycling.

The so-obtained TOKAM3X-EIRENE package was first applied to analyse qualitatively the impact of neutral recycling on edge plasma turbulent transport. Pairs of simulations in circular limited and diverted geometries were run, with in each case a simulation including self-consistently neutral recycling compared to a reference simulation in which turbulence was driven by a prescribed core particle in-flux (Figure 4). As was expected, neutral particles ionization in the vicinity of target plates was observed to be the dominant drive of particle fluxes in these simulations. This change of topology for the particle source (from core to target plates) has an immediate consequence on the phenomenology of transverse heat fluxes in the edge plasma [Tamain, NFxxxx]. As seen in Figure 5, the change of localization of the particle source leads to an increase of the weight of the conductive component of the energy flux compared with the convective part. This trend is particularly striking in the inner part of the simulations domain but is also visible, although milder, in the outer part. These results bring new insight in the debate on the nature of transverse heat transport in the edge plasma. Simulations also show that neutrals recycling perturb fluctuations properties in the vicinity of target plates (increase of intermittency mainly) whereas they remain qualitatively unchanged away from them.

It must be stressed that these results apply only for the parameter regime explored for these first studies and will have to be checked when scanning divertor regimes. Indeed, the inclusion of self-consistent neutral particles physics in the TOKAM3X code opens of whole new area of investigations for the analysis of heat exhaust and H-mode physics and gives an edge to the TOKAM3X code in that field with respect to its main competitors.

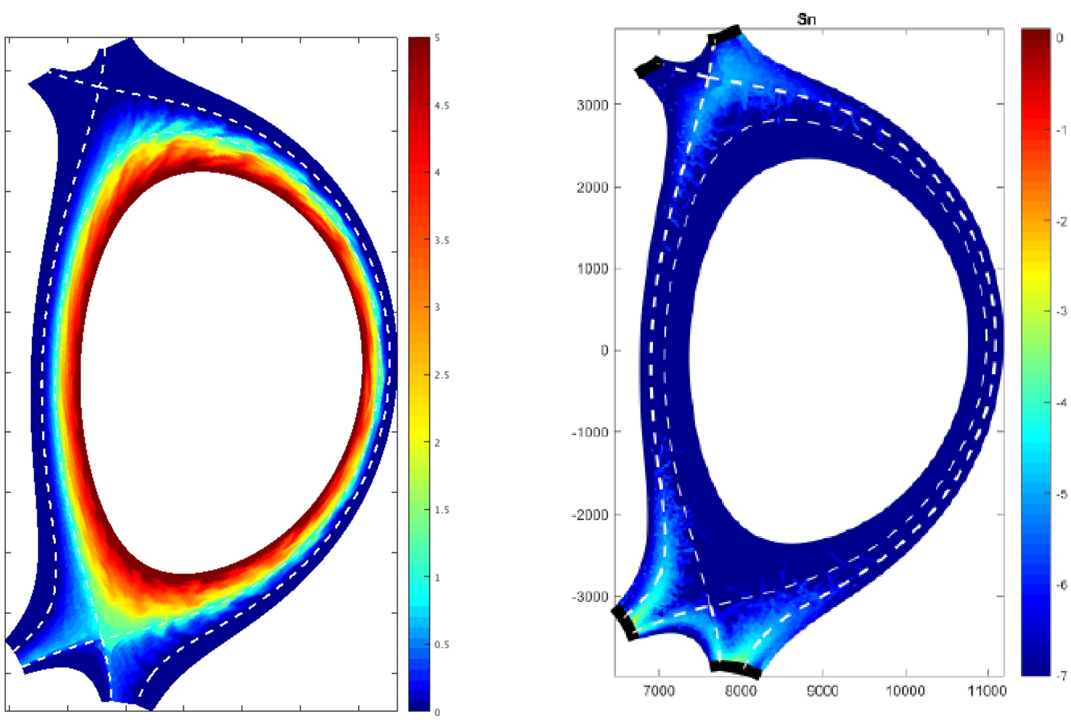

Figure 5: poloidal plane snapshots from a simulation in WEST divertor configuration of: left – the total density field including turbulent fluctuations (dimensionless units); right - the volumetric particle source driven by neutrals recycling (log scale, arbitrary units).

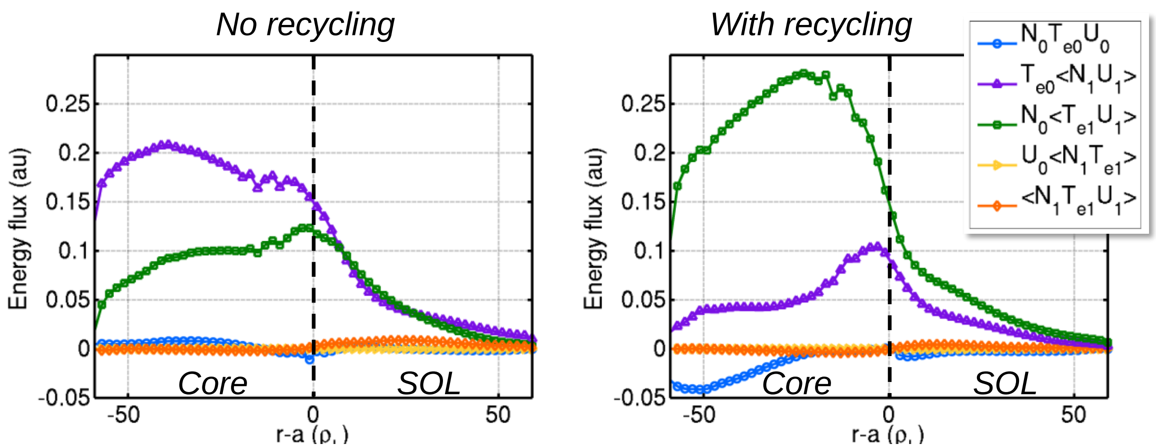

Figure 6: radial profile of the radial electron energy flux decomposed in its various components. Left: simulation without neutral particles recycling included (same as Figure 4). Right: simulation including neutral particles recycling.

3.5. References

[Asakura, JNM2007] "Understanding the SOL flow in L-mode plasma on divertor tokamaks, and its influence on the plasma transport", N. Asakura and ITPA SOL and Divertor Topical Group, Journal of Nuclear Materials 363–365, 41-51 (2007).

[Bufferand, NF2015] "Numerical modelling for divertor design of the WEST device with a focus on plasma–wall interactions", H. Bufferand et al., Nucl. Fusion 55, 053025 (2015).

[Carralero, NF2014] "An experimental investigation of the high density transition of the scrape-off layer transport in ASDEX Upgrade", Nucl. Fusion 54, 123005 (2014).

[Colin, JNM2015] "Impact of the plasma-wall contact position on edge turbulent transport and poloidal asymmetries in 3D global turbulence simulations", C. Colin et al., J. Nucl. Mater. 463, 654-658 (2015).

[Goldston, NF2012] "Heuristic drift-based model of the power scrape-off width in low-gas-puff H-mode tokamaks", Nucl. Fusion 52, 013009 (2012).

[Kukushkin, JNM2011] "Physics requirements on fuel throughput in ITER", A.S.Kukushkin et al., Journal of Nuclear Materials 415, S497-S500 (2011).

[Loarte, NF2007] "Chapter 4: Power and particle control [Progress in the ITER Physics Basis (PIPB)]", A. Loarte et al., Nucl. Fusion 47, S203 (2007).

[Tamain, CPP2014] "3D Properties of Edge Turbulent Transport in Full Torus Simulations and their Impact on Poloidal Asymmetries", P. Tamain et al., Contrib. Plasma Phys. 54, 555-559 (2014).

[Tamain, PPCF2015] "Multi-scale self-organisation of edge plasma turbulent transport in 3D global simulations", P. Tamain et al., Plasma Phys. Control. Fus. 57, 054014 (2015).

[Wagner, PPCF2007] "A quarter-century of H-mode studies", F. Wagner, Plasma Phys. Control. Fusion 49, B1-B33 (2007).

[Zweben, PPCF2007] "Edge turbulence measurements in toroidal fusion devices", S. J. Zweben et al., Plasma Phys. Control. Fusion 49, S1–S23 (2007).

3.6. Publications and Presentations of TOKAM3X results involving EoCoE work

Publications in peer reviewed journals

[Baudoin, CPP2018] "Turbulent heat transport in 3D edge plasma simulations", C. Baudoin et al., Contributions to Plasma Physics 58, 484-489 (2018).

[Baudoin, PhD2018] "Numerical evaluations of mechanisms governing the heat transport in the edge plasma of tokamaks", PhD Thesis, Aix-Marseille University (2018).

[Fan, CPP2018] "Self-consistent coupling of the three-dimensional fluid turbulence code TOKAM3X and the kinetic neutrals code EIRENE", D.-M. Fan et al., Contributions to Plasma Physics 58, 490-496 (2018).

[Fan, NME2018] "Effect of turbulent fluctuations on neutral particles transport with theTOKAM3X-EIRENE turbulence code", D.-M. Fan et al., Nucl. Mater and Energy, submitted (2018).

[Galassi, NF2017] "Drive of parallel flows by turbulence and large-scale ExB transverse transport in divertor geometry", D. Galassi et al., Nucl. Fusion 57, 036029 (2017).

[Galassi, PhD2017] "Modélisation numérique du transport et de la turbulence dans le plasma de bord des tokamaks avec géometrie magnétique point-X", PhD Thesis, Aix-Marseille University (2017).

[Gallo, PPCF2018] "Impact of the plasma geometry on divertor power exhaust : experimental evidence from TCV and simulations with SolEdge2D and TOKAM3X", A. Gallo et al., Plasma Physics and Controlled Fusion 60, 014007 (2018).

[Tamain, JCP2016] "The TOKAM3X code for edge turbulence fluid simulations of tokamak plasmas in versatile magnetic geometries", P. Tamain et al., J. Comput. Phys. 321, 606-623 (2016).

[Tamain, NFxxxx] "Impact of self-consistent neutrals dynamics and particle sources on edge plasma transport and turbulence in 3D first principle simulations", P. Tamain et al., to be submitted to Nuclear Fusion.

International conferences and workshops:

C. Baudoin et al. "Drift driven vs turbulent heat transport in 3D edge plasma simulations", poster at the 16th plasma Edge Theory conference, Marseille (2017).

D.-M. Fan et al. "Effect of particle fueling and recycling on the properties of SOL and Edge turbulent fluctuations in global TOKAM3X-EIRENE simulations", poster at the 16th plasma Edge Theory conference, Marseille (2017).

D.-M. Fan et al. "Effect of turbulent fluctuations on neutral particles transport with theTOKAM3X-EIRENE turbulence code", poster at the 23rd Plasma Surface Interactions conference, Princeton (2018).

D. Galassi et al. "Analysis of SOL flows in diverted and limited plasmas with 3D global turbulence simulations", poster at the PSI conference, Roma (2016).

D. Galassi et al. "Impact of diverted geometry on turbulence and transport barrier formation in 3D global simulations of tokamak edge plasma", invited talk at the 8th IAEA technical Meeting on Theory of Plasma Instabilities, IAEA Headquarters, Vienna (2017).

D. Galassi et al. "Impact of diverted geometry on turbulence and transport barriers formation in 3D global simulations of tokamak plasma edge", poster at the 44th EPS conference on plasma physics, Belfast (2017).

A. Gallo et al. "Impact of the plasma geometry on divertor power exhaust : experimental evidence from TCV and simulations with SolEdge2D and TOKAM3X", invited talk at the 44th EPS conference on plasma physics, Belfast (2017).

F. Nespoli et al. "3D modelling of transport and turbulence in the WEST divertor", contributed talk at the EFTSOMP workshop, Prague (2018).

P. Tamain et al.	"Impact of magnetic geometry and X-point configuration on edge plasma turbulence and transport in 3D first principle simulations", invited talk at the 16th plasma Edge Theory conference, Marseille (2017).
P. Tamain et al.	"Impact of self-consistent neutrals dynamics and particle sources on edge plasma transport and turbulence in 3D first principle simulations", invited talk at the 23rd Plasma Surface Interactions conference, Princeton (2018).